Experimental evaluation of timber-
-to-timber connections using wood dowels

Bárbara Daniela Monteiro Pereira

UMinho | 2016

Universidade do Minho
Escola de Engenharia

Bárbara Daniela Monteiro Pereira

Experimental evaluation of timber--to-timber connections using wood dowels

November 2016

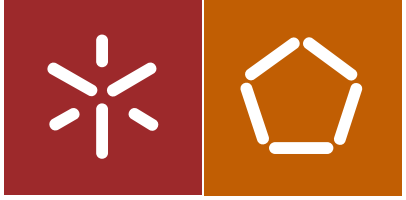

Universidade do Minho
Escola de Engenharia

Bárbara Daniela Monteiro Pereira

Experimental evaluation of timber--to-timber connections using wood dowels

Master Thesis
Integrated Master in Civil Engineering

Work conducted under the supervision of
Professor Jorge M. Branco

November 2016

"Specifying wood in public procurement can help fulfil national and local climate change programmes. Encouraging the use of wood products can act as a greener alternative to more fossil-fuel intensive materials. Substituting a cubic metre of wood for other construction materials (concrete, blocks or bricks) results in the significant average of 0.75 to 1 t CO_2 savings."

International Institute for Environment and Development, Using Wood Products to Mitigate Climate Change, 2004

This page intentionally left blank.

Acknowledgments

I would like to express my gratitude to my advisor, Prof. Jorge Branco for his guidance and support. Thank you for your teaching, experience and friendship.

To the companies that showed interest in my project and provided the material. I am truly grateful to AOF, Portilame and StoraEnso. Without the support of these strong engineering companies this work would never have been possible to achieve.

There are many important contributors that have made it possible to achieve this work. I am grateful to César, Matos and Marco for their support during the experimental work performed at the Laboratory of Structures of the University of Minho. I am also grateful to all the remaining staff of the Laboratory sections for their help and for the funny moments that provided me with were crucial for me to keep up the good mood even in those "lesser good" days that we all have.

For the precious technical guidance, I want to thank the post-doc researchers from the University of Minho's timber study group.

To my colleagues that have undertaken this academic journey with me: Bárbara, Cátia, Joana Machado, Zé, Maria João, Miguel, Sara Barbosa and my newest wood partner Jorge Barros! Thank you all for your support and for the incredible moments we had and hopefully will continue to have!

To Cristina Barroso, for the long days we have spent in the laboratory and in the library working hard! Together we made a great team. I wish, with all my heart, the best the world can give you.

To my best friends, Ana Paula, Ana Rita and Susana. From you all I learnt the true meaning of friendship!

I am also grateful to Dra. Alexandrine and Juliana for their friendship, support and good advices.

A special thanks to my boyfriend, Vítor Faria, who was always there for me during the good and lesser good moments of my life and never allowed me to give up my dreams. Thank you for your patience with me. Without you those would be some dark times!!

To my grandparents who spoiled me and helped to make me the person that I am today.

Last but not the least, to my parents without whom I would never have achieved anything in life. You always let me choose my path and when I fell you were the first to pick me up and showed me the right way. You showed me that with effort, honesty, respect and love nothing is impossible.To my sister, who I love, thank you even when you nagged me!

Thank you all!!

Abstract

Nowadays an increase of interest in wood as a construction material is being noticed and also in old structural timber elements strengthening, mostly due to the principal characteristic of wood that is sustainability.

With this in mind, it was found important to evaluate timber to timber connections with wood dowels instead of the most current: steel dowels. For this purpose, two engineered products were used, namely glue laminated timber or glulam and cross laminated timber, also called as CLT (both made of Norway spruce). Concerning the inherited old buildings chestnut was chosen since it is the most common species found in Portuguese historical timber buildings. As a dowel it was decided to use two types of material: laminated venner lumber or LVL, that was proposed by a Scandinavian company (StoraEnso); and massaranduba timber due to its behavior in a series of experiments conducted in the University of Minho where the main goal was not the dowel behavior but instead the global joint performance. Therefore, five types of experiments were performed: three with the goal to increase the knowledge about massaranduba mechanical characteristics, namely compression characterization, dowel-bearing strength and yield moment and embedment strength. To finalize double shear tests were performed in order to have knowledge about the failure mode of that type of fastener. The wood dowel dimension was the same in all experiments, 12 mm.

The conducted experiments showed that the massaranduba dowel is a viable option for steel. Nevertheless, more experiments need to be done to create a large database with reliable results. However, the LVL dowel with 12 mm of diameter is not a viable option due to its failure.

Keywords: wood dowels, glulam, CLT, chestnut, embedment strength, double shear.

This page intentionally left blank.

Resumo

Atualmente tem sido notado um aumento do interesse na madeira como material de construção e também no reforço de elementos estruturais de madeira, principalmente devido à principal característica da madeira que é a sustentabilidade.

Com isto em mente, achou-se importante avaliar as ligações do tipo madeira-madeira com cavilhas de madeira ao invés das mais utilizadas: cavilhas de aço. Para este propósito, dois produtos de engenharia foram usados, nomeadamente, *glue laminated timber* ou glulam, e *cross laminated timber* também chamado de clt (ambos feitos de abeto norueguês). No que diz respeito aos edifícios herdados, optou-se pelo castanho visto que é a especie mais comummente encontrada nos edificios históricos de madeira em Portugal. Como cavilha decidiu-se usar dois tipos de material: *laminated venner lumber* ou LVL, que foi proposto por uma empresa escandinava (*StoraEnso*); e massaranduba devido ao seu comportamento numa série de ensaios realizados na Universidade do Minho nos quais o principal objectivo não foi a comportamento da cavilha mas sim o desempenho global das ligações. Por isso, foram realizados cinco tipos de ensaios: três com o objetivo de aumentar o conhecimento acerca das características mecânicas da massaranduba, nomeadamente, caracterização da compressão, do esmagamento localizado da cavilha e resistência de rotação; caracterização da resistência ao esmagamento localizado da madeira; e para finalizar realizaram-se testes de duplo corte por forma a ter conhecimento do modo de ruptura da cavilha. Foi usada a mesma dimensão diametral da cavilha em todos os ensaios, respectivamente, 12 mm.

Os ensaios realizados mostraram que a massaranduba é uma opção viável para o aço. No entanto, mais experiências necessitam de ser efetuadas com o intuito de criar uma base de dados com resultados fiáveis. Contudo, a cavilha de LVL com 12 mm de diâmetro não é uma opção viável tendo em conta a sua ruptura frágil.

Palavras-chave: cavilhas de madeira, glulam, clt, castanho, esmagamento, duplo corte.

This page intentionally left blank.

Contents

This page intentionally left blank.

List of Figures

This page intentionally left blank.

List of Tables

This page intentionally left blank.

Chapter 1

Introduction

1.1 General

Timber structures belong to the past, present and future of humanity. Our ancestors left us an incredible heritage concerning wood buildings around the world and as an example of longevity of this type of construction we have the archaeology study which dates the first timber framing joints in the Far East and Europe around 200 B.C. In India, timber shaped from teak was found, connected with simple joinery and bamboo pegs. It is also said that the Golden Hall (1.1(a)) and the Pagoda (1.1(b)) Japanese monuments, dated from the sixth century are the oldest monuments still standing in the world (Benson, 1981).

(a)

(b)

Figure 1.1: Timber buildings in Japan dated from the sixth century: a) the Golden Hall of the Horyu-ji Buddhist temple;[1] b) the three-storied pagoda of the Hokki-ji Buddhist temple.[2]

On the other hand, wood construction began to decrease with the expansion of other materials while the knowledge on timber joints started to vanish with the abandonment of the construction of timber buildings. That happened, for example, in Portugal with a significant reduction in the use of timber structures. And with this abandonment, an important part of the know-how was lost and, therefore, with the lack of knowledge, incorrect interventions became more common. One usual mistake is related with the inappropriate joints strengthening in terms of stiffness and/or strength (Branco, 2008). As such, the lack of knowledge of the behavior of timber joints made the professionals prefer the use of simpler materials like steel and to substitute original timber joints by steel based solutions. This increases the economic value of restoration and in extreme cases the idea of restoration is abandoned and the building destroyed.

The interest in timber restoration and in new construction is growing due to several facts (comfort, aesthetics, security and sustainability, etc.). With this in mind, researches of the behaviour of timber elements and joints is increasing. However, when compared with other construction materials, wood is less studied than it should be and so, this project idea had arisen focusing on dowel type fasteners, on the less studied ones, such as wood dowels. Thereby, the main challenge will be to understand the distribution of forces inside the dowel.

For the development of this work, three companies - AOF, Portilame and Stora Enso - gently provided the Norway spruce, chestnut, CLT, and massaranduba samples which were used for testing in the Laboratory of Structures of the University of Minho.

1.2 Motivation

Nowadays a global increasing environmental awareness is being noticed and the proof is the Paris Climate Conference (COP 21) in December 2015. The first universal climate agreement has been approved, with 195 countries committing to the target of keeping the global rise in temperature below 2°C. One of the most important things to do in order to contribute to that global target is to reduce the fossil carbon dioxide emissions. The most effective ways to do this are improve renewable energy efficiency (like biomass or solar panels) and renewable materials (like wood-based products).

In comparison with other materials, like steel and concrete, wood as a construction material contributes efficiently to this purpose due to its carbon dioxide zero emissions.

[2]source:https://upload.wikimedia.org/wikipedia/commons/2/2f/T%C5%8Ddai-ji-Kond%C5%8D.jpg

[2]source:https://upload.wikimedia.org/wikipedia/commons/e/ed/Horyu-ji09s3200.jpg

In other words, trees produce oxygen and sequester carbon dioxide as they grow, which is stored during the life of the building (Energy, 2010).

However, it cannot go unsaid that the use of wood as a construction material needs to be in accordance with our forest, otherwise we will only be contributing to the increase of the climate change problem. With this in mind, organizations like FSC[3]and SFI[4], among others, play a crucial role in an effective forest management.

After some years, wood construction started to reappear, peaking the interest of building companies around the world. As such, new constructions appeared and restoration increased without modifying the characteristic material of the structures,but a problem continues to exist: the over dimension of the weakest points of timber structures, connections, which renders the design economically less attractive.

Bearing all this in mind, the following idea appeared: why not use wood as a mechanical fastener instead of steel? And so, the present project came to life. Wherefore, wood dowel connections will be studied experimentally to increase the know-how about this type of connections and contribute to the academic research as, for example, Sawata and Yasumura (2002) and Milch et al. (2016) already gave, hoping to improve the global knowledge on this matter.

1.3 Objectives

The aim of this thesis is to provide additional knowledge about the behavior of wood implemented as a mechanical fastener in timber-to-timber connections by trying to understand the forces distribution inside the fastener. Therefore, a theoretical and preliminary study was performed followed by an experimental assessment that will help to verify rules set in EN-1995-1-1 (2004) are applicable to wood dowels. This way, goals of the experimental campaign are: assess the compression capacity of timber used as dowel; evaluate the dowel bearing strength; estimate the embedment strength of the mechanical fastener; identify the failure mode in double shear, recognize that the desirable mode is the one with two inflection points corresponding to ductile failure. In order to complement the study a comparison will be made between wood and steel dowels to estimate and compare the results of the embedment strength.

[4]Forest Stewardship Council; independent, non-governmental organization established to promote responsible management of the world's forests and is probably the most well-known forest certification program worldwide

[4]Sustainable Forestry Initiative; is based on the premise that responsible forest practices and sound business decisions can co-exist

Moreover, it is a personal goal to increase the degree of knowledge on this subject, to contribute to the research carried out at the University of Minho and help increase the global knowledge about the behavior of connections with wood dowels.

1.4 Document Structure

The present dissertation is divided into five chapters including the present one. A brief description of them is given next.

Chapter 2

In this chapter, the knowledge obtained with all bibliography read about conventional timber connections that was crucial to go ahead with this project will be explored. It will consist of three main sections: the first one addresses the issue of carpenter joints, the second one will present some knowledge about glued joints and finally, the third one describes the acquired knowledge about connections with mechanical fasteners.

Chapter 3

Chapter 3 presents some curiosities about the material used and in it the adopted procedure for each experiment will be described. The experimental campaign will be divided into three phases, each one regarding test typology. There are four sections concerning the experiments.

Chapter 4

After the experimental campaign, a description will be necessary to explore the results obtained in the laboratory. For this purpose, chapter 4 consists of presenting and discussing all data. As such, it will be divided into four sections, each one regarding the typology of test the adopted.

Chapter 5

Finally, conclusions will be taken and some considerations will be given about the general results and the applicability of EN-1995-1-1 (2004) principles in wood dowels design. In addition, and because it is important to continue exploring connections and mechanical fasteners behavior, a section about future work will also be presented.

Chapter 2

Conventional Timber Connections

2.1 Introduction

This chapter has the purpose to present the state of knowledge achieved during the bibliography research on timber-to-timber connections, more precisely, dowel type connections.

Timber construction is an ancient way to build shelters and it is even considered by Herzog et al. (2004) and Benson (1981) as the oldest building material of all. Connections between structural elements play an important role in any structural wood system mostly due to their capacity to transfer loads along the components (Snow et al., 2006). Moreover, joints require special attention in order to ensure the global security of the given elements that are subjected to local stresses and also because connections behavior is conditioned by physical and mechanical factors.

Conventional connections will be the explored theme. As such, there are three principal types of conventional timber connections to discuss: carpentry joints, glued joints and joints with mechanical fasteners. In this last one, emphasis will be given to so-called dowel type connections taking into consideration that this is what the present project is all about.

2.2 Carpentry joints

There is a large variety of carpentry joints with structurally distinct variants of the same type depending on the geographic location and period of time. This variability

is related mainly to function, type, structural behavior and shape of joints. Therefore, some studies across the world have been made in order to create a database of historic carpentry joints improving the assessment of timber structures and also to contribute to new construction design taking into account their behaviour (e.g. Ehlbeck and Larsen (1993), Erman (1999), Sobon and Schroeder (2012), Serafini et al. (2016)).

For example, Sobra et al. (2015) proposed preliminary taxonomy of historical carpentry joints divided into two principal groups: within members and between members. The first group includes scarf joints (tension and compression) and coupling joints; the second group takes into consideration different angles and consequently different shapes. Moreover, they observed that identical joints have multiple names in different countries and regions, thus, in the authors taxonomy proposal it is also recorded the name given to the joint typology in question (see figure 2.1(a) where it is presented a non-exhaustive scheme of that proposal).

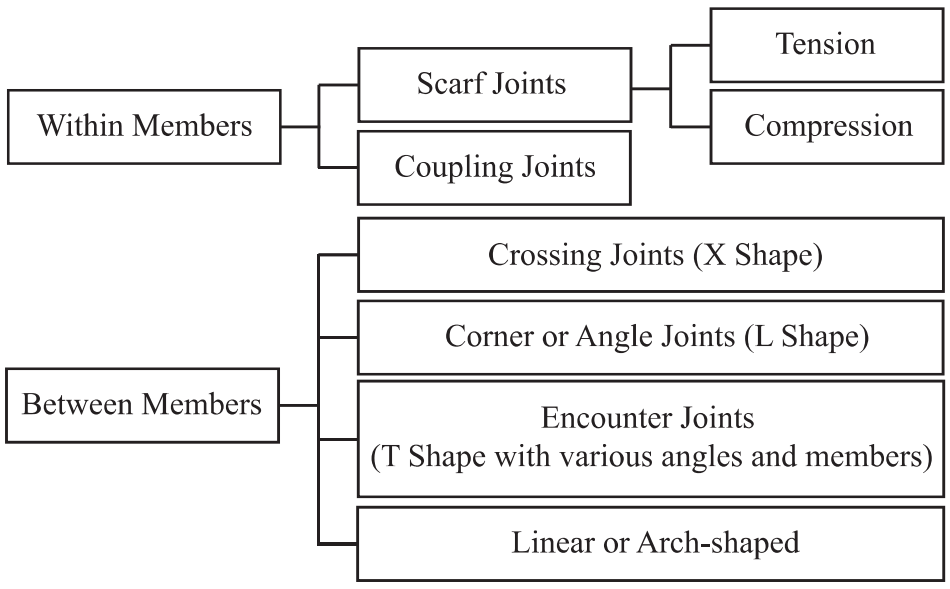

(a)

Figure 2.1: Taxonomy proposal for historic carpentry joints (Adopted from Sobra et al. (2015)).

More generally, Branco and Descamps (2015) categorized old timber carpentry into four main types according to their arrangement and geometry: mortise and tenon joints, notched joints, lap joints and scarf joints. For mortise and tenon, authors specified two types: "L" shape and "T" shape. The first configuration can be analysed in figure 2.2(a), where two possible ways to build can be seen. From up to down, it is represented the through pinned mortise and tenon in which the tenon passes the

total mortise length, and the blind pined mortise and tenon where the tenon length is shorter than the mortise length. The second configuration, presented in figure 2.2(b), is divided into two different configurations. From left to right it can be seen through tenon with outside wedges and, on the right illustration, wedged and pined dovetail.

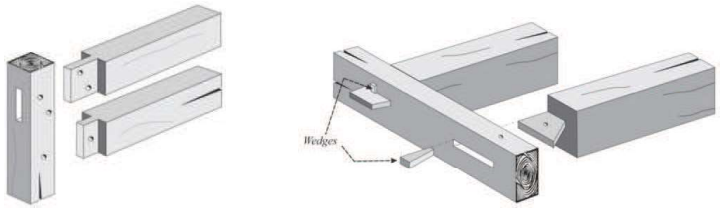

(a) (b)

Figure 2.2: Mortise and tenon: a) trough pined and blind pinned configuration; b) with outside wedges and wedged and pined dovetail (Branco and Descamps, 2015).

As far as notched joints are concerned, (see figure2.3), Branco and Descamps (2015) referred to them as being to the development of king post and king post-like frames. As seen in figure 2.3(a), a notch consists of a "V" shaped groove commonly perpendicular to the length of the beam that supports the whole element creating the strength of the joint. Notwithstanding, a tenon can be added to this type of joint (2.3(b)) with the purpose of keeping the elements coplanar. According to Parisi and Cordié (2010), this type of connection is also called as single-step birdsmouth joint and is often adopted in various nodes of roof trusses and can also be found in reverse configuration, as shown in figure 2.3(c) and with double-step, as presented in figure 2.3(d).

(a) (b) (c) (d)

Figure 2.3: Notched joints: a) between main rafters and tie-beam; b) peak joint with a notched joint; c) reverse configuration; d) double-step joint (Branco and Descamps, 2015), (Barbosa, 2015).

Additionally, the third joint referred above is the lap joint presented in figure 2.4. By analysing it is visible that different variants from the same joint exists. If the elements are mounted without removing any material from them it is considered as a full lap joint and elements are normally assembled with a pin (see figure 2.4(a)).

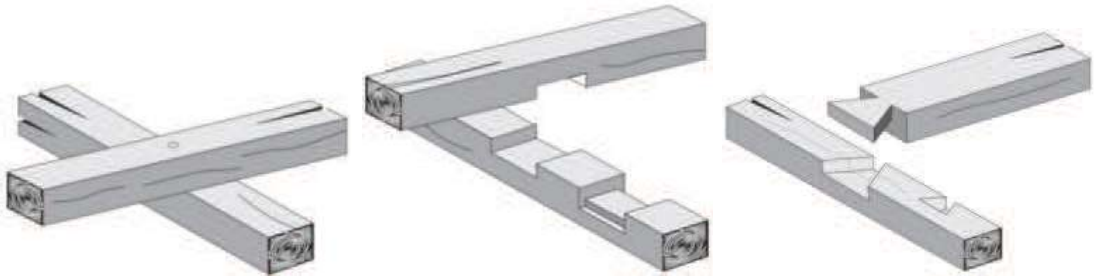

(a) (b) (c)

Figure 2.4: Lap joints: a) full lap joint (pinned); b) half-lap joint and cogged half-lap joint; c) through dovetailed lap joint and wedged dovetailed lap joint (Branco and Descamps, 2015).

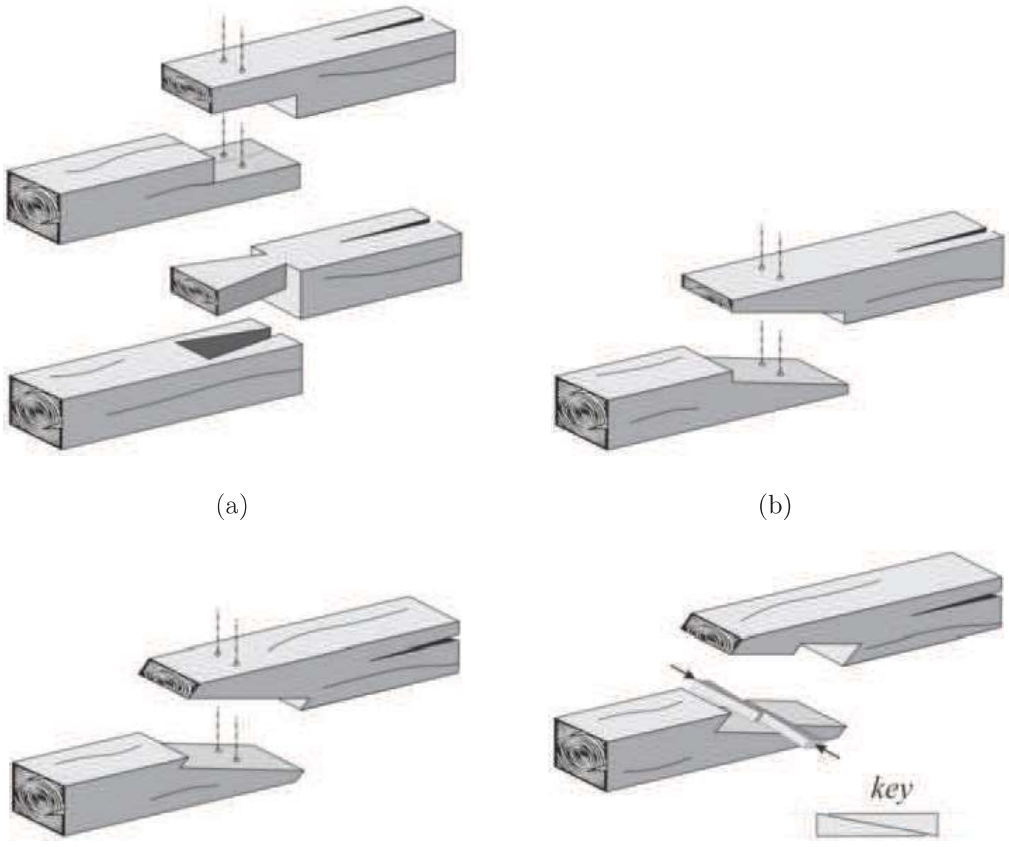

(a) (b)

(c) (d)

Figure 2.5: Scarf joints: a) halved (or half-lap splice joint) and lapped dovetail; b) scarf joint; c) under-squinted ends scarf joint; d) *Trait de Jupiter* or French scarf joint with wedges (key) (Branco and Descamps, 2015).

Otherwise, when thickness is removed, usually half of the thickness in each member, the joint is called half-lap joint or cogged half-lap joint when cogs exist, as shown in

figure 2.4(b). At last, looking at figure 2.4(c), another typology is presented as dovetail lap-joint. This one can be mounted through the member or embedded in the element.

Scarf joints (2.5) are normally used when the member does not have the length required to the joinery in construction. As said by Sobra et al. (2015), this type of joint increases length within members. In figure 2.5(a) it is represented a common halved scarf joint and a lapped dovetail where the first consists in a lap whose surfaces are parallel to the members, and consequently also called as half lap joint with co-axial members and the second is known as a half-lapped joint with the lapped portions shaped as a dovetail joint, owing its name because of that. Figures 2.5(b) and 2.5(c) presents a common scarf joint and a scarf joint with under-squinted ends, respectively. There is also a particular scarf joint with wedges where the presence of the key is essential, known as French scarf joint or *Trait de Jupiter* or bolt of lightning (see figure 2.5(d)). To finalize, and because Japanese joints are one of the most ancient ones in timber buildings, four types of joints from this culture will be presented. They are known by Tanahashi and Suzuki (2016), as the major types of traditional timber joints in Japan which are *Nuki*, *Yatoi*, *Sashi-gamoi* and strut joints.

According to Fujita et al. (2016), *nuki* can be called penetrating beam or batten and it was introduced in Japan by China in the 12^{th} century. Thus, the penetrating beam consists in an horizontal element that penetrates the column through a hole. In some cases a wedge is used to tighten the joint (see figure 2.6).

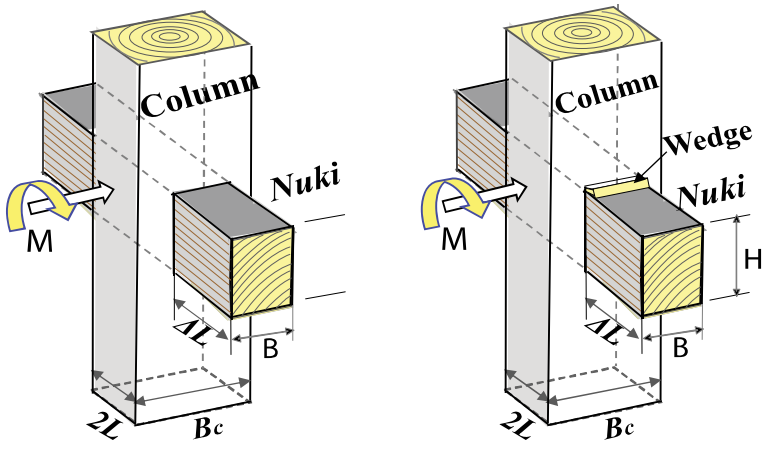

(a) (b)

Figure 2.6: *Nuki* type connection: a) without wedge; b) with wedge (Tanahashi and Suzuki, 2016).

Therefore, in figure 2.7 it is represented the *yatoi* joint detailed by Tanahashi and Suzuki (2016). Authors referred to this connection as "employed tenon" due to the

combination of separated beams that are mounted in column by a sandwiched system. The *shachi-sen* mechanism detailed in the same figure has an identical function to a cotter, a type of shear connector.

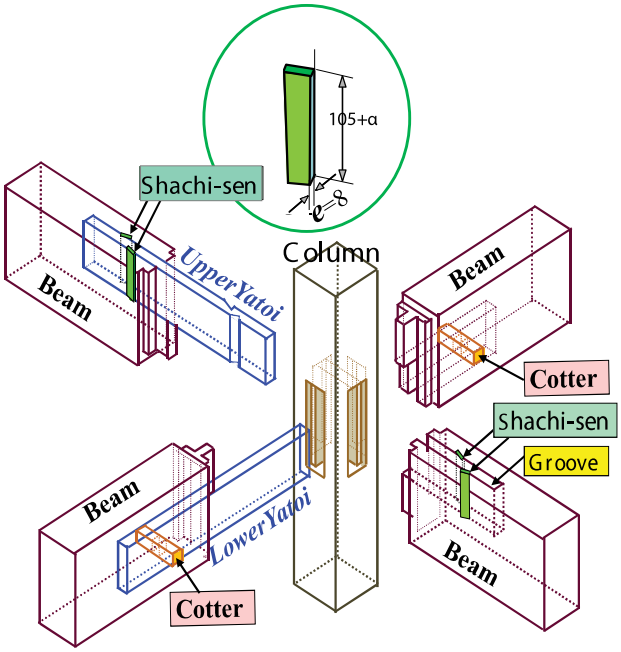

Figure 2.7: *Yatoi* joint (Tanahashi and Suzuki, 2016).

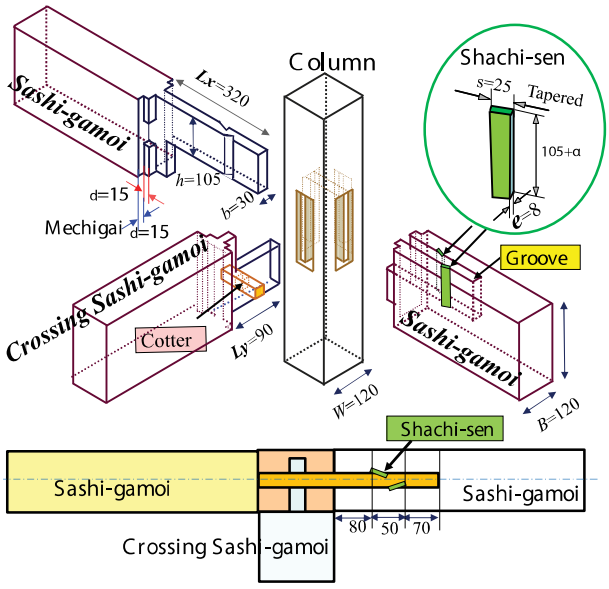

Figure 2.8: *Sashi−gamoi* joint details (Tanahashi and Suzuki, 2016).

Sashi-gamoi (see figure 2.8) also means "an inserted lintel" (Tanahashi and Suzuki, 2016) and according to the authors it has been developed by combining the *nuki* with

the lintel or the lintel with tenons. A part of the resistance of the joint is given by the *sashi-gamoi* tenon that goes through the crossing tenon and in contact with the column surface appears an reaction between the "tenon" and the "face mortise wall".

Strut type joint is divided by two mechanisms, A and B, shown in figure 2.9. In the first mechanism, as seen in figure 2.9(a), the strut is supporting the floor beam and in the second mechanism, represented in figure 2.9(b), the strut stays between the upper beam and the lower beam (Tanahashi and Suzuki, 2016).

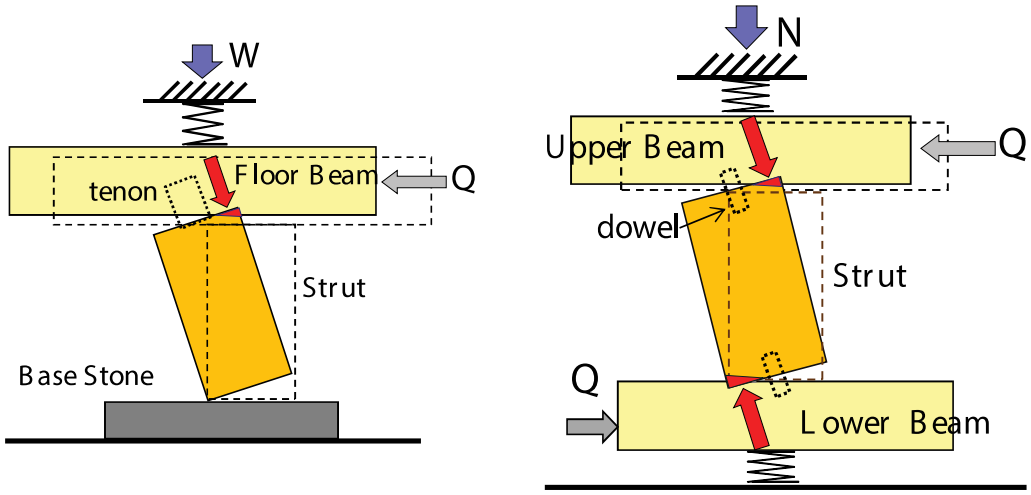

(a) (b)

Figure 2.9: Strut type joint: a) detail of mechanism A; b) detail of mechanism B (Tanahashi and Suzuki, 2016).

2.3 Glued joints

Many studies have been performed to assess the resistance component of adhesives used in glued joints and their durability. There are several ways to apply glue in timber connections. Adhesives could be used for gluing old carpentry types of joints, bond rods through timber elements, rehabilitation and repairing techniques, modern timber engineering like glued laminated timber (glulam).

As to glulam, this is considered by Ross et al. (2010) as one of the oldest glued engineered wood products. This technology consists on gluing two or more layers of lumber with layers parallel to length or perpendicular to the adjacent lamellas (cross lamination). In fact, there has been a strong investigation about cross laminated timber (CLT) due to its many advantages, including the two directions strength rather than one direction, only in the case of simple glulam improving the anisotropy of wood. More

recently, in March 2016, some researchers met in Stockholm to discuss value, challenges and necessary developments of CLT for the next years (see Falk et al. (2016)). LVL or laminated venner lumber is another form of glulam, consisting in a layered composite of wood veneers (usually with 3mm thickness) that are bonded together under heat and pressure. According to Malo et al. (2016) the Treet building, localized in Norway, is the tallest timber building in the world, with 14 storeys, and glulam was used in timber beams as the main structural material (see figure 2.10). Thus, this kind of construction shows the potentialities of glulam as a structural element.

(a)

(b)

Figure 2.10: a) detail of a structural glulam beam b) Treet building.[1]

For Batchelar and Mcintosh (1988), structural joints can cost from 5% to in excess of 50% of the value of un-jointed glulam members. As such, the McIntosh Timber Laminates Ltd introduced the glue cross-lapped joints as commonly referred in New Zealand as McIntosh joint, which is mounted in factory by gluing and cross-lapping or interleaving multiple timber members (see figure 2.11). This type of joints load transfer is made by means of shear at the glue interfaces and the authors even referred to that method as the efficient one at developing full strength rigid moment resisting joints.

[1]source: http://treetsameie.no/

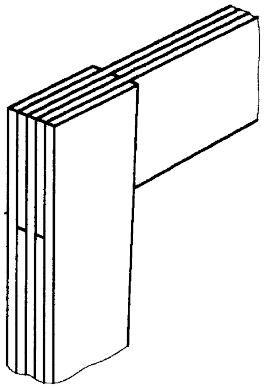

Figure 2.11: Glued cross-lapped joint detail (Batchelar and Mcintosh, 1988).

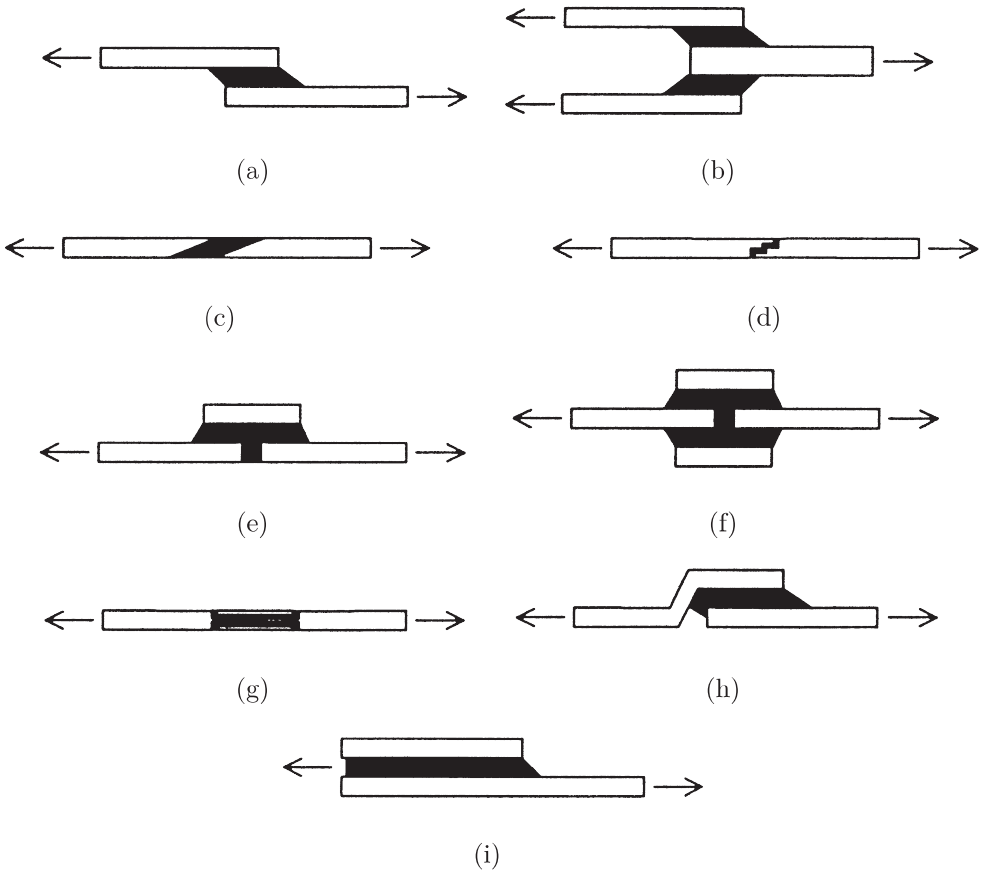

Figure 2.12: Common adhesively bonded lap joints: a) single lap; b) double lap; c) scarf; d) step; e) butt strap; f) butt double strap; g) recesses double strap; h) joggle lap; i) lap shear (Tong and Steven, 1999).

(a) (b) (c)

Figure 2.13: Common adhesively bonded butt joints: a) butt; b) landed scraf tongue and groove; c) tongue and groove (Tong and Steven, 1999).

Conrad et al. (2007) present a brief review of literature about fracture of wood composites and wood-adhesive joints. They conclude that the behaviour of adherends is important and, according to the literature reviewed, the researchers, in their majority, concluded that fracture of wood adhesive joints should not occur at the wood-resin interface for maximum performance. Examples of usual structural adhesive bonded joints are shown in figures 2.12 and 2.13 with the purpose of easily understand the joint fracture behaviour.

Numerical and experimental investigation was performed by Tannert et al. (2012) on adhesively bonded full-scale double-lap joints composed of timber adherends (spruce) and adhesive layers. Three parameters were investigated: the thickness of the adhesive layers (0,5 mm-2,0 mm), the overlap length (40 mm-280 mm), and the ductility of the adhesive (using three different adhesives). The experimental results suggested that the joint strength is independent of adhesive investigated layer thickness, increases with the overlap length up to an maximum apparent of 200 mm, and is almost independent of the adhesive stiffness. The authors had a good agreement between the numerical and experimental results.

More recently, Nicolaidis et al. (2016) performed some research trying to fill the gap about knowledge on fire resistance of adhesively bonded timber joints. A series of temperature tests, at a range of $20°C$ to $150°C$, with single lap joints were conducted in order to understand the failure mode changes with increasing bond line temperatures and, at the same time, the observation of bond line splitting and normal force peeling. They concluded that with the increase of temperature, the failure mode changes from timber to cohesion failure, emphasizing the importance of further investigations about this subject to enhance the knowledge.

Another applicability of glue in timber connections is by means of rods glued-in through members. In this case, a large investigation is being made nowadays in order to improve this type of connections. This type of joint is a kind of hybrid between glued joints and joints with mechanical fasteners. According to Serrano (2000), glued-in rods have been used mostly in Scandinavia and Germany with a method divided normally

in to two principles. The first one, frequently used in Sweden, consists in drilling an oversized hole into the timber or glulam member, inject an amount of adhesive and afterwards insert a threaded rod. Then, when the rod is pressed into the hole, the adhesive overflows indicating that the inserted amount of adhesive was sufficient. Whereas, the other method consists in drilling a hole smaller than the nominal diameter of a threaded rod which in comparison with the first method contains also a lengthwise groove, and then a second hole is drilled perpendicular and close to the bottom of the first hole. After that procedure, the rod is screwed into the timber and the adhesive is injected through the second hole until it pours out at the free end of the rod. There is no need for a special equipment to produce glued-in joints. However, it has to be done in a factory environment and with proper adhesives to obtain reliable connections.

In 2008, Madhoushi and Ansell (2008a) and Madhoushi and Ansell (2008b) performed to types of tests with glued-in GFRP[2], pultruded rods bonded into the epoxy resin. In the first test, they focused on describing the static fatigue behavior of in-line beam to beam connections, which were connected with three rods configuration and its mechanical behavior compared with solid unjointed LVL. The authors concluded that solid LVL beams have significantly higher static and fatigue strengths compared with beams jointed with GFRP glued-in rods. However, the experiments showed that solid LVL beams have lower capacity to dissipate energy under cyclic loads than jointed beams. Furthermore, in the second part of the experiments, two types of jointed structure were studied, beginning with an L-shaped moment-resisting LVL structure containing two members at a right angle and finishing with a U-shaped LVL frame containing three members. Both, L-shaped and U-shaped frames had two GFRP pultruded rods bonded into the members with epoxy resin adhesive. In this part of the test series, they concluded that L-shaped structure has a longer life as the magnitude of the constant amplitude fatigue stresses are reduced. On the other hand, U-shaped frames, loaded under simulated earthquake cycle with increasing amplitude of displacement, showed a pattern of damage initiation of steady state growth and failure reflected in the trends in hysteresis loop area, viscous damping and dynamic modulus. Summarizing, connectors showed good ductility and capability to dissipate energy under dynamic loading.

Recently, Hunger et al. (2016) carried out a series of experimental pull-compression tests with glued-in steel rods in glulam and LVL of different timber species (Norway spruce, European ash and European beech) with the set up described in figure 2.14. The rod diameter and the anchorage length were maintained constant for the elastic

[2]Glass fibre-reinforced plastic

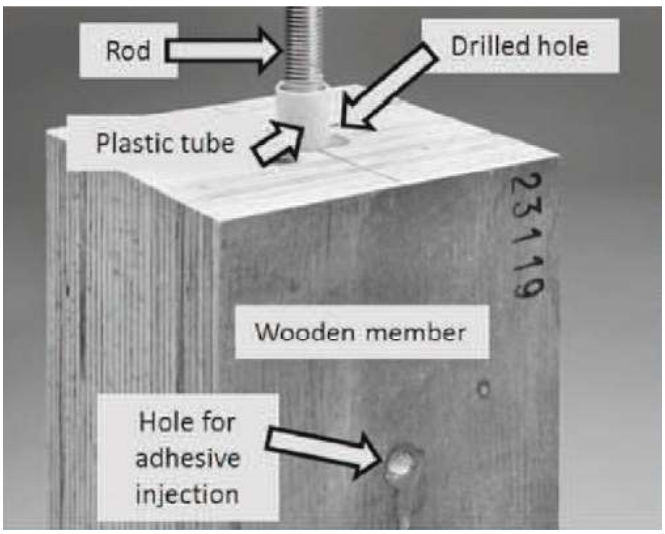

Figure 2.14: Detail of pull-compression test with glued-in rods (Hunger et al., 2016).

and elastic-plastic behavior characterization. Their idea was to show the applicability of glued-in rods both in softwoods and glulam members as well as in hardwood and in wood-based products like LVL.

Taking into account that the present project is focused in the study on wood dowels type of connectors the author considered relevant the exposure of two investigations made with glued-in wood dowels. The fist study, carried out by Jensen et al. (2004), focused on investigating the moment-resisting capacity of hardwood dowels glued-in parallel to grain with theoretical principles validated by experimental tests. They used glulam beams made of Japanese cedar (*Cryptomeria japonica*) and dowels made of hard maple (*Acer saccharum*). After the pure bending tests, pure shear tests and combined bending and shear tests (some specimens were tested in a 3-point bending test set-up, in which the location of the joint varied in order to obtain different combinations of moment and shear force) were performed, the authors concluded that hardwood dowels glued in parallel to grain with diameter about 12 mm may produce joint strength competitive with conventional glued-in steel rod joints. In addition, they developed simple models based on fracture mechanisms enabling easy and rotational design for pure bending and pure shear actions that were in a good agreement with tests results. This way, the substitution of steel or aluminium by hardwood dowels is viable where ductility behavior is required.

Still in 2004, Pizzi et al. (2004) performed a series of tests slightly different from the others previously described concerning about the bonding type. In this case, the dowel was bonded by high speed rotation, without the use of any adhesive (see figure 2.15). This technique showed that the use of dry dowels, inserted hot in the substrate

after preheating them at high temperature ($100°C$), yielded consistently better results than PVAc[3]gluing.

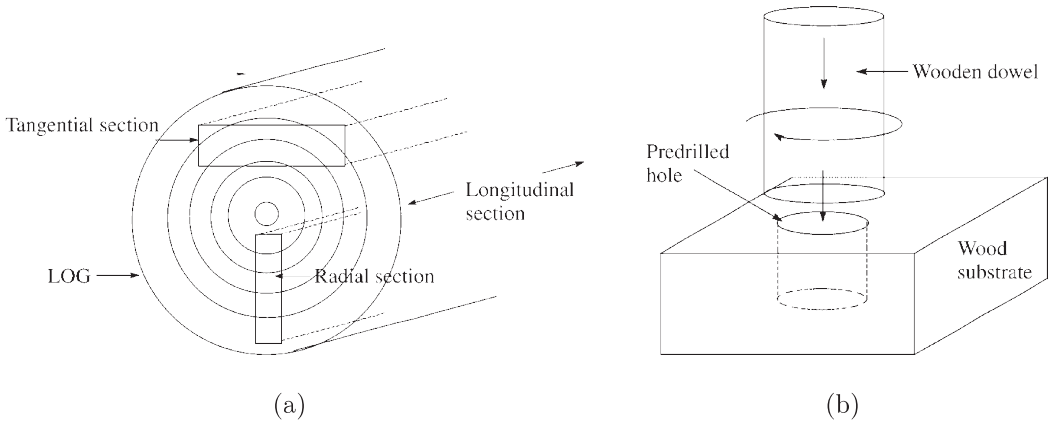

Figure 2.15: Detail of dowel bonding by high-speed rotation: a) tangencial, radial and longitudinal sections of used dowels; b) insertion wood dowel in a pre-drilled hole in wood substrate (Pizzi et al., 2004).

2.4 Joints with mechanical fasteners

Joints with mechanical fasteners is the generic name given to dowel-type connections. In fact, these are the most common joints in timber-to-timber connections and this term is referred generally to nails, screws, bolts, and properly so called dowels. These connectors are normally subjected to bending and shear and the load transfer is due to connector bending, diametric pressure and shear along the wood member length.

The design of dowel-type connections is based on the theory of plasticity first formulated by K. W. Johansen in Johansen (1941) and Johansen (1949). This theory originated the European Yield Model (EYM) that is present nowadays in EN-1995-1-1 (2004) and allows the determination of load bearing capacity of connectors between two or three wood members, based on stress equilibrium applied on the inserted connector through the wood element In other words, the ultimate load bearing capacity of a single connector is predicted when either the stresses in the wood reaches the plastic failure stress level or when a combination of plastic failure in wood element and dowel is attained. Besides the simplicity of this method, the application in the complex behavior of dowel-type connections represents high reliability in practical quantification of load bearing capacity. The embedment strength of timber and the yield moment of the fastener are two material parameters, besides geometrical parameters, essential to

[3]Polyvinyl acetate

calculate the load-carrying capacity of timber joints with mechanical fasteners. This theory validation was later verified through extensive and comprehensive experiments carried out by Wilkinson (1972), McLain and Thangjitham (1983), Whale and Smith (1986), Soltis et al. (1986), Ehlbeck and Werner (1992), Hübner et al. (2008) and more recently Brühl et al. (2011), among others.

Milch et al. (2016) performed a series of experimental and numerical analyses with the aim to describe the non-linear behaviour of wood. For this purpose, the authors used Norway spruce (*Picea abies L. Karst.*) and European beech (*Fagus sylvatica L.*) and tested it to compression parallel and perpendicular to the grain, three point bending and double shear joints following ASTM-D2395 (2014), BS-373 (1957), EN-383 (2007) and EN-26891 (1991) standards principles. For the finite-element (FE), analyses took into account the orthotropic elasto-plastic material behaviour with isotropic non-linear hardening. The numerical model and the experimental results had a good agreement with a relative error of 16%, meaning that the proposed elasto-plastic material models are reliable and could contribute to future design of wood structures and its performance. Figure 2.16 shows the comparison between experimental and numerical results of wood dowel failure, where UY represents the displacement in load direction, EPPLXY means shear plastic strain in RT plane of dowel, and EPPL1 represents the first principal plastic strain distribution of the dowel. R is the sample dimension in the radial direction (mm) and T is the sample dimension in tangential direction (mm).

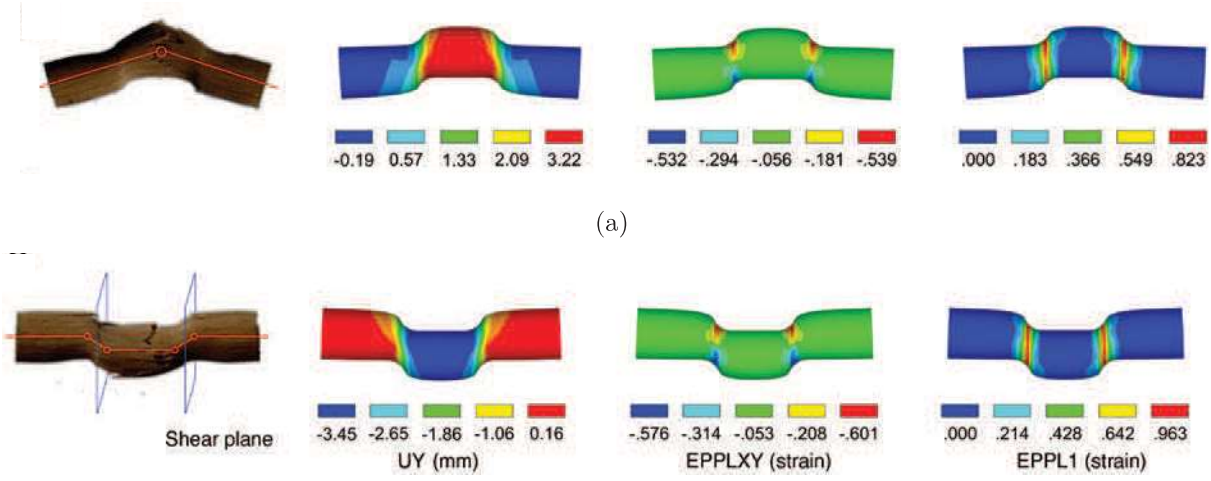

Figure 2.16: Experimental and numerical dowel failure tested parallel to the grain: a) double-shear with European beech dowel tested in tensile; b) double-shear with European beech dowel tested in compression (Milch et al., 2016).

Sawata and Yasumura (2002) produced a database of embedding strength of wood for the design of dowel-type joints, based on the results obtained by an extensive experimental campaign with embedding tests and compressive tests parallel and perpendicular to the grain. The authors evaluated the results according to two different methods: 5% offset method and a maximum load up to 5 mm displacement as reported in EN-383 (2007). For this purpose, authors used two types of specimens: ezomatsu (*Picea jezoensis Carriere*) and todomatsu (*Abies sachalinensis Fr. Scmidt*) which had four grades (L90, L100, L110, L125), according to Standard (2003), and dowels with diameters of 8 mm, 12 mm, 16 mm and 20 mm. With that study there conclusions were divided into four principle topics, quoting:

1. The coefficient of variation of the embedding strength from all lamina grades varies from 10% to 17% and 15% to 21%, respectively, in the parallel and perpendicular directions. There is a significant correlation between embedding strength and density.

2. The embedding strengths parallel to the grain evaluated by the 5% off-set method and the maximum load up to 5 mm displacement according to EN383 shows close values that are scarcely influenced by dowel diameter. The embedding strength perpendicular to the grain evaluated by the 5% off-set method is little influenced by dowel diameter as well. However, the embedding strength evaluated by the maximum load up to 5 mm displacement decreases as the dowel diameter increases.

3. Embedding strength evaluated by the 5% off-set method can be estimated from the dowel diameter and the density of the wood. The design value of embedding strength in the EN-1995-1-1 (2004) standard is useful for the embedding strength evaluated by the maximum load up to 5 mm displacement according to EN-383 (2007).

4. The embedding strength for the dowel-type fastener can be estimated by Eqs.2.1 to 2.3 using the compressive strength parallel to the grain of wood.

Embedding strength parallel to the grain:

$$fh_{0,5\%} = fh_{5mm} = 0,9fc_0 \tag{2.1}$$

Embedding strength perpendicular to the grain:

$$fh_{90;0,5\%} = 0,4fc_0 \tag{2.2}$$

$$fh_{90;5mm} = (-0,016d + 0,745)fc_0 \tag{2.3}$$

where $fh_{0,5\%}$ and fh_{5mm} are the embedding strengths (MPa) parallel to the grain evaluated by the 5% off-set method and the maximum load up to 5 mm displacement according to EN383, respectively, $fh_{90;0,5\%}$ and $fh_{90;5mm}$ are those perpendicular to the grain, respectively, fc_0 o is the compressive strength (MPa) parallel to the grain, and d is the dowel diameter (mm).

Sandhaas et al. (2013) reported the results of 139 embedment tests parallel to grain according to EN-383 (2007). The materials used in the experiments were dowels with different steel grades and diameters (12 mm and 24 mm) and five wood species (including two European species and three tropical hardwood species) with different moisture contents and random densities. According to the authors, the tests results showed that EN-1995-1-1 (2004) equation for predicting the embedment strength penalizes wood species with higher densities in contrast with the overestimation of species with lower densities. In addition, they also observed a lower influence of the dowel diameter and even proposed an equation (2.4) adapted from the existing in EN-1995-1-1 (2004), solely based on wood density which, according to them, would be sufficient and easier for structural engineers to handle in practical situations.

$$f_{h,0} = 0,082\rho \tag{2.4}$$

where $f_{h,0}$ means embedment strength and ρ means density.

As to the wood ductility, Sandhaas et al. (2013) observed a significant difference between the species tested, most probably because of their anatomy. As regards the density, authors proposed to include adjustments of the embedment strength to the moisture contents in EN-383 (2007). As for dowels, they remained elastic apart from the strong influence of the used steel grades which may be due to their different hardness and, as a consequence, originated different friction coefficients.

Šobra et al. (2016) performed a series of experimental tests carried out in the University of Minho. Within this framework, dovetail joints, with and without dowels, were tested under compression and tension and then the experimental results for the load bearing capacity were compared with analytical values. For joint members, they used Scots Pine *Pinus sylvestris* and Maritime Pine *Pinus pinaster*, for dowels massaranbuba *Manilkara spp.* timber was used and assumed to be strength class D60. They noticed that joints with dowels seemed to triple the load-bearing capacity, both in compression and tension. Concerning experimental and analytical values

obtained, for dovetail joint without dowel the values were quite accurate, unlike those with dowel. For dovetail joints with massaranduba dowels the analytical models are underestimated.

2.5 Final Remarks

There are several studies about conventional timber-to-timber connections among the citations in the previous sections, including recent investigations. However, from this brief literature review for the reader's sake of mind it was only emphasized the investigations that the author of the present document found important to her research.

To sum up, besides the large investigation on the subject of dowel-type fastener, comparing with steel dowels, less importance is given to wood dowels, which consolidates the relevance of the present project.

In addition, the last research presented formed the basis line for the current project due to the unexpected results and failure condition of massaranduba dowels.

This page intentionally left blank.

Chapter 3

Experimental Program and Materials

3.1 Introduction

The present chapter will be divided in two main sections: materials and experimental campaign. In the first one, some wood characteristics, concerning the chosen materials will be very briefly presented, whereas a brief explanation of all tests performed, used standards and ways to obtain the principal results to discuss in Chapter 4 will be given in the second section.

3.2 Materials

For the development of this work, the most common material present in Portuguese historical timber buildings was taken into account - chestnut - and the most common nowadays in modern timber buildings and proposed to be studied by StoraEnso renewable materials company - glulam, CLT and LVL. These products were made of Norway spruce. Because of the well-known properties of glulam and CLT less focus will be given in this chapter in order to keep it brief and organised.

Concerning the used dowels, it was decided to evaluate hardwood and steel so that a comparison can be made between the two different materials. Massaranduba was chosen to be studied due to material performance in a series of experiments carried out in the University of Minho by Šobra et al. (2016).

In addition, while waiting to test the samples, they were all accommodated in a climatic chamber at 20 ± 2 degrees Celsius and approximately 65% ± 5% of humidity.

Despite the great characteristics of LVL, when used as 12 mm dowels, it does not work efficiently. One embedment test with LVL dowel was performed and the failure happens at the moment of the application of a 0,2 kN pre-load (the same in all experiments with massaranduba and steel dowel). For that reason, LVL dowels experiments were not performed and it was found unnecessary to present any result in the present dissertation.

3.2.1 Spruce

Spruce (*Picea abies*) is the most abundant conifer in Europe (of Threatened Species, 2016), as such, it is assessed as Least Concern by IUCN Red List of Threatened Species[1]and is not listed in the CITES[2]Appendices. Moreover, the Norway spruce is widely planted for its wood, and is the species used as the main Christmas tree in several cities around the world.

According to Mitchell (1972), trees may reach 25 m to 55 m and bark is deep copper-brown or rich red-brown, with pale, fine shreds rubbing off. Its trunk dimensions are approximately from 1 cm to 1,5 cm. The cones are cylindrical, tapering towards the tip, slightly curved, 15 cm to 20 cm long, with leathery scales, pendulous at shoot-tips. Figure 3.1 there are shown images of the spruce tree and details of the cross section.

(a) (b)

Figure 3.1: Spruce tree: a) tree; b) detail of a trunk and bark.[3]

The glulam provider set the wood strength class as GL24h corresponding to 380

[2]International Union Conservation of Nature
[2]Convention on International Trade in Endangered Species of Wild Fauna and Flora
[3]http://bioweb.uwlax.edu/bio203/s2009/madisen-neil/ (retrieved on November 2016)

kg/m^3 of mean density, according to EN-1194 (1999). Whereas the CLT samples provider set the wood strength class as C24 which corresponds to 420 kg/m^3 of the mean density according to EN-338 (2003).

3.2.2 Chestnut

Chestnut (*Castanea sativa Mill*) is one of the most common species found in Portuguese historical timber structures. The main difference between this specie and spruce is that chestnut is a hardwood, unlike spruce and its wood-based products that are softwood. Is not listed in the CITES Appendices and in IUCN Red List of Threatened Species.

In addition, trees may attain 20 m to 35 m height, with a net-shaped pattern bark and deep fissures passing spirally in both directions up the trunk (see figure 3.2). The leaves, that provide food for some animals, are oblong-lanceolate shaped and hardily toothed, and may reach 10 cm to 30 cm long and 4cm to 10 cm wide.

(a) (b)

Figure 3.2: Chestnut tree: a) tree;[4]b) detail of a trunk cross section.[5]

D40 was the strength class given by the supplier company, and taking into account EN-338 (2003), chestnut mean density is 700 kg/m^3.

3.2.3 Massaranduba

Massaranduba (*Manilkara spp*) or bulletwood is widespread in tropical and semitropical locations. It is rated as being very durable, with good resistance to most insect

[5]http://jb.utad.pt/especie/castanea-sativa (retrieved on November2016)
[5]https://upload.wikimedia.org/wikipedia/commons/a/aa/Castanea-sativa-MHNT.BOT.2006.0.1272.JPG (retrieved on November2016)

attacks and susceptible to marine borers. It has good workability but may pose some challenges in gluing, mostly due to high density and oil content.

This type of wood is not listed in CITES Appendixes neither in IUCN Red List of Threatened Species which makes it desirable to work with.

3.3 Experimental Campaign

So as to understand dowel and element behavior, four types of experiments were made according to European and Portuguese standards. The experimental campaign and respective norms are described in the next subsections.

For all tests, the equipment used had the capacity to apply and continuously record the load to an accuracy of ± 1% of the load applied to the test piece. Moreover, the equipment had the capacity to continuously record the displacement of the fasteners in the wood with an accuracy of ± 1%.

3.3.1 Compression characterization of wood dowels

In order to know the compression capacity of wood used as dowel (Massaranduba), the principles and test set-up in Portuguese standard 618 were taken into account. As such, the equipment has the capacity to apply forces until 200 kN with less than 1% of error. Concerning the samples, they all had, approximately, cross section dimension (20 mm x 20 mm) and length (50 mm) (see figure 3.3), were knot-free and without any other types of visual flaws.

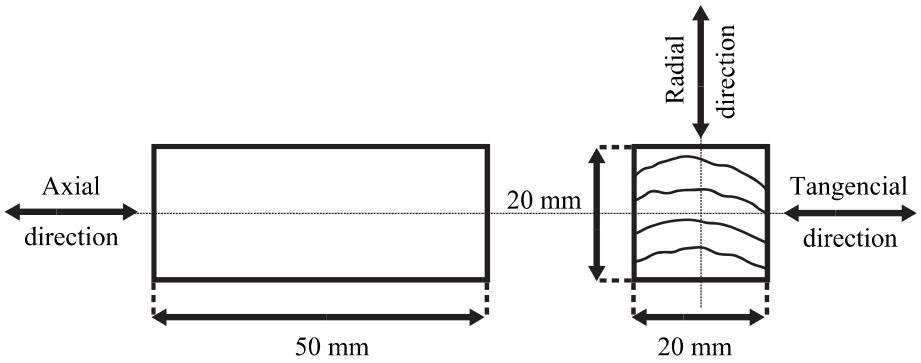

Figure 3.3: Massaranduba samples details (Adapted from IGPAI (1973).

The applied test procedure was prepared according to principles described in IGPAI (1973). As a result, the test was performed with the grains parallel to load, with special

attention to specimens basis that were strictly perpendicular to their axis. Thereupon, increasing compression stress was applied at a constant rate of 0,017 mm/s, with 200 kN load cell, until rupture occurred between three and four minutes after the test started. Hence, the maximum load applied corresponds to the rupture strength of the samples. One LVDT[6]was also used, placed in the loading head of the test machine, measuring thereby the grain displacement presented by specimens so that conclusions could be taken. In addition, the compression strength parallel to grain is given by equation 3.1 presented strictly downwards.

$$f_{c,o} = \frac{F_{max}}{bh} \tag{3.1}$$

The set-up as well the equipment used and a real sample tested can be seen in figure 3.4.

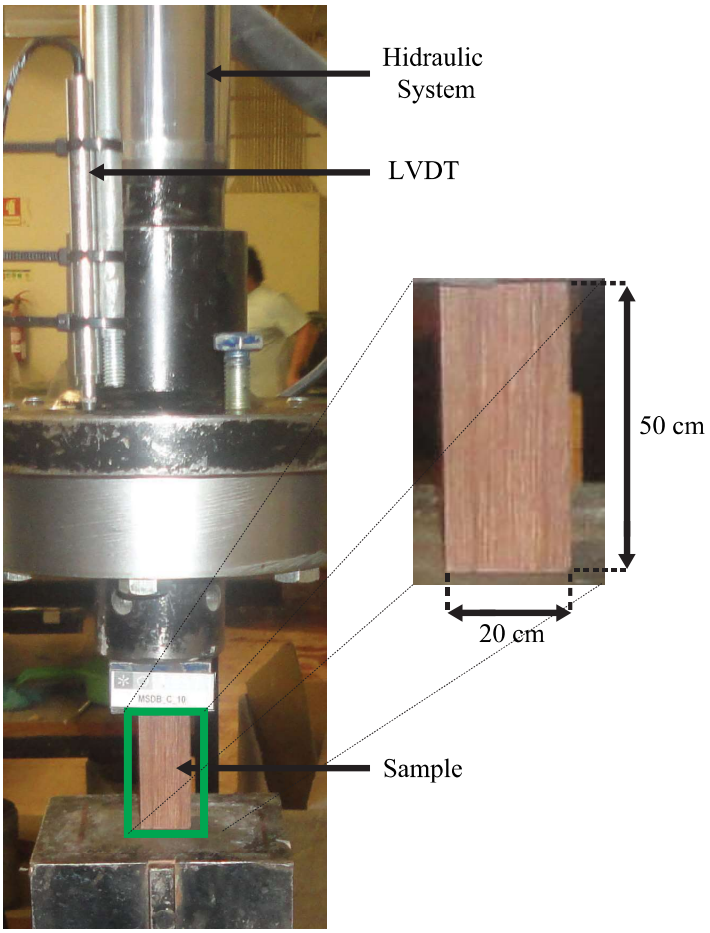

Figure 3.4: Test set-up.

[6]Linear Variable Differential Transformer

3.3.2 Dowel-bearing strength

This type of test was performed in order to evaluate the behaviour of the fastener inside the joint. With this in mind, the setting proposed by Schmidt (2006) was taken into account to do the test procedure. For this purpose, massaranduba dowels were used, with 12 mm of diameter and length of 80 mm as shown in figure 3.5.

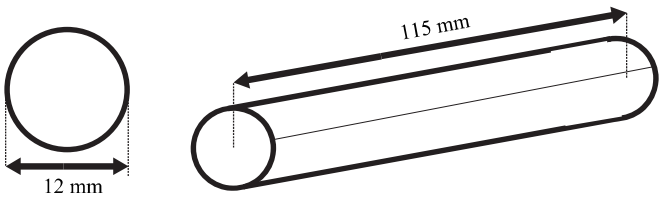

Figure 3.5: Dowel dimensions.

The test set up had a steel block with the same dimensions as the timber used in the embedment tests with the difference in order to know the mechanical behaviour of the dowel, it was only necessary to use a block with half of the dimensions. After all set up in the test equipment, as can be seen in figure 3.6, the dowel was subjected to compressive load perpendicular to the grain, oriented in radial direction with maximum confinement and applied on half circumference. Tests were conducted on a testing machine at a uniform deformation rate of 0,017 mm/s, while loads and deformation were measured at various intervals.

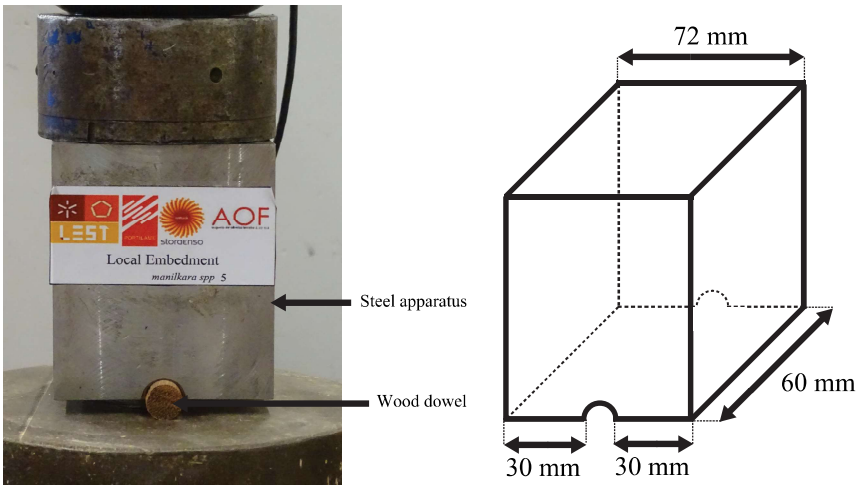

(a) (b)

Figure 3.6: Details of set apparatus: a) test set up; b) steel block.

3.3.3 Embedment strength of dowel type fasteners

The embedment strength or embedding strength is defined by EN 383 (EN-383, 2007) as, and quoting, the average compressive stress at maximum load in a piece of timber or wood based sheet product under the action of a stiff linear fastener. The fastener's axis is perpendicular to the surface of the timber. The fastener is loaded perpendicular to its axis. This parameter can be quantified by two different methods, according to experiments described in EN-383 (2007), where the embedment strength is divided in parallel and perpendicular tests, or analytically with the expressions exposed in EN-1995-1-1 (2004).

The test piece, consisting of a rectangular prism of wood with a fastener placed with its axis perpendicular to the surface of the prismatic test piece, had its dimensions calculated based on figure 3.7 and table 3.1.

Table 3.1: Sizes of test pieces. (Adapted from EN-383 (2007), table 1, page 8)

Measurement	Bolts and dowels
a1	3d
l1	7d
l2	7d

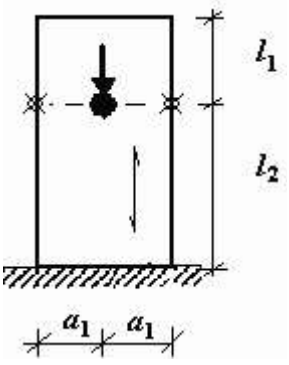

Figure 3.7: Test piece dimensions as specified in Table 3.1 with transducer pick up points

According to the test principle described in EN-383 (2007), the steel apparatus had to be done in conformity with the wood piece, resulting in a steel apparatus and wood member as shown in 3.8(b) Other metallic pieces had to be made to support the LVDT's.

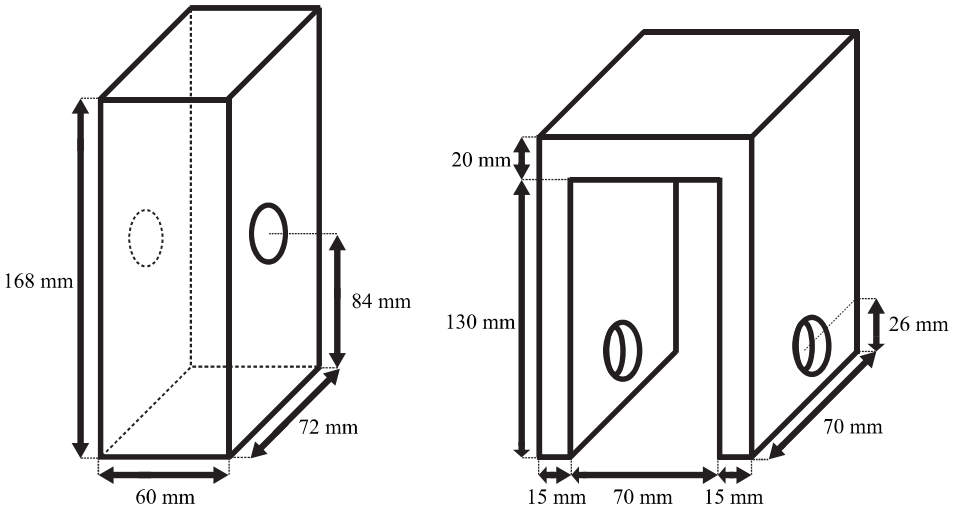

(a) (b)

Figure 3.8: Illustration of test pieces: a) test principle; b) steel apparatus.

The test was carried out using the apparatus from figure 3.9, was always prepared in a way so as to avoid bending of the fastener under test.

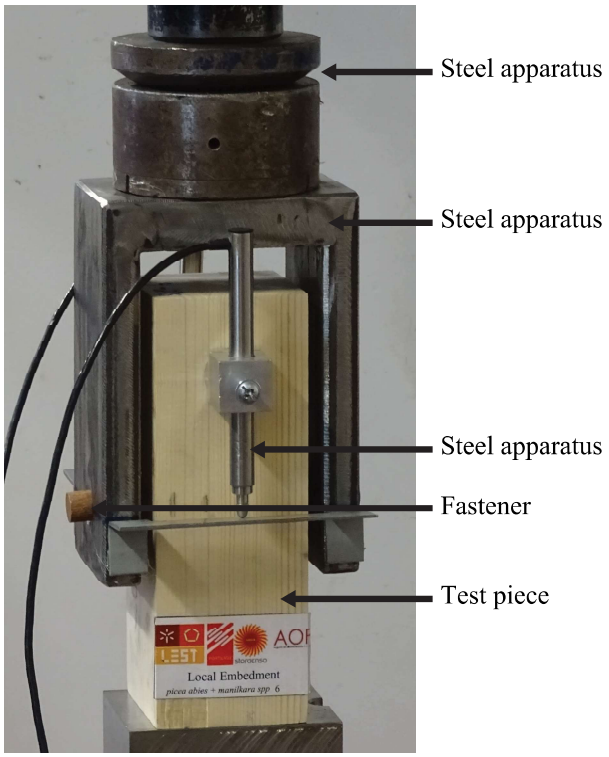

Figure 3.9: Samples dimensions.

Test procedure

The following procedure followed the principles described in EN-383 (2007). Wherefore, the test piece was placed symmetrically in the test apparatus so that the load could be applied in the axis of the test piece.

Moreover, the relative displacement of the dowel-type-fastener in respect to the test specimen was measured between the steel apparatus that holds the dowel and points on the edges of specimens, at the level of the centre line of the dowel. Two displacement transducers were placed on opposite edges.

The estimated maximum load $F_{max,est}$ was determined on the basis of a preliminary test. For each series of tests, the first experiment had to be monotonic in order to know the maximum force estimated, with a constant rate of 0,017 mm/s and displacement control. The procedure was then the following: the load increased to 0,4 $F_{max,est}$ and maintained for 30 sec. Then the load was reduced to 0,1 $F_{max,est}$ and maintained for 30 sec. Thereafter, the load increased and the test stopped when the deformation reached 15 mm.

The load increased and decreased at a constant rate of loading-head movement.

In addition, this process was used for two different types of dowel: massaranduba and steel. For each one of them, three types of wood were used as member, glulam, chestnut and cross laminated timber, which made a total of seventy-two tests

Calculations

Taking into account the principles contained in EN-383 (2007), the embedding strength shall be calculated to an accuracy of 1% using the following formula:

$$f_h = \frac{F_{max}}{dt} \tag{3.2}$$

where, $f_{h,est}$ is the estimated embedding strength, in N/mm^2; f_h is the embedding strength, N/mm^2; $F_{max,est}$ is the estimated maximum load, in N; F_{max} is the maximum load, N; d is the fastener section dimension, in mm; and t is the thickness, in mm.

Design equations

According to EN-1995-1-1 (2004) the embedment strength parallel to grain is given by equation 3.3,

$$f_{h,0} = 0,082(1 - 0,01d)\rho \tag{3.3}$$

with, $f_{h,0}$ as the embedment strength parallel to grain (N/mm^2), ρ as the timber

density (kg/m^3), and d as the dowel diameter (mm).

3.3.4 Yield moment

According to EN-409 (2009), the yield moment given by the experimental results corresponds to the bending moment when the specimen is deformed through a prescribed rotation angle and the yield moment is given by,

$$M_y = max \begin{cases} F_1 \times l_1 \\ F_3 \times l_3 \end{cases} \tag{3.4}$$

where, F_1 and F_3 are the maximum support loads on the dowel, l_1 and l_3 are the distances between loading points and the nearest support.

To better understand the set-up configuration see figure 3.10

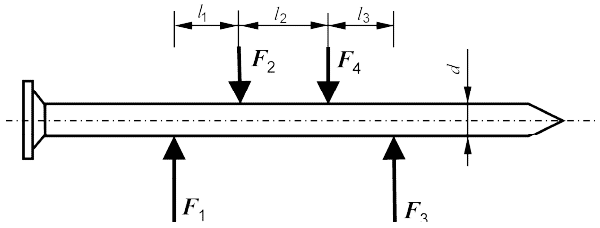

Figure 3.10: Detail of yield moment test set-up (EN-384, 2004).

Design formulas

On the other hand, according to EN-1995-1-1 (2004) the yield moment for bolts is given by equation 3.5:

$$M_{y,Rk} = 0,3 f_{u,k} d^{2,6} \tag{3.5}$$

where, $M_{y,Rk}$ is the characteristic value for yield moment (N.mm), $f_{u,k}$ is the characteristic tensile strength (N/mm^2), and d is the bolt diameter (mm).

Therefore, the characteristic tensile strength will be calculated according to equations 3.6 and 3.7. Knowing $f_{c,0,k}$ from compression characterization tests, $f_{m,k}$ can be calculated and then by its substitution in equation 3.6 the characteristic tensile strength ($f_{t,0,k}$) is known. Consequently, $f_{t,0,k}$ value will substitute $f_{u,k}$ in equation 3.5 in order to get to know $M_{y,Rk}$ for massaranduba dowels.

$$f_{t,0,k} = 0,6 f_{m,k} \tag{3.6}$$

$$f_{c,0,k} = 5(f_{m,k})^{0,45} \tag{3.7}$$

With, $f_{t,0,k}$ as the characteristic value of tensile strength parallel to grain in N/mm^2, $f_{m,k}$ as the characteristic value of bending strength in N/mm^2, and $f_{c,0,k}$ as the characteristic value of compression strength parallel to grain in N/mm^2.

3.3.5 Double shear with wood dowels

With the aim to better understand the behaviour of a timber-to-timber connection with mechanical fastener (more specifically, wood fastener), which is the main goal of the present project, specifications and principles in EN-1995-1-1 (2004) and EN-26891 (1991) had to be taken into account. Beginning with the experimental analyses,

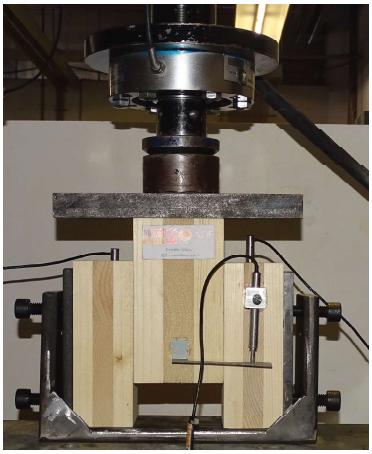

(a)

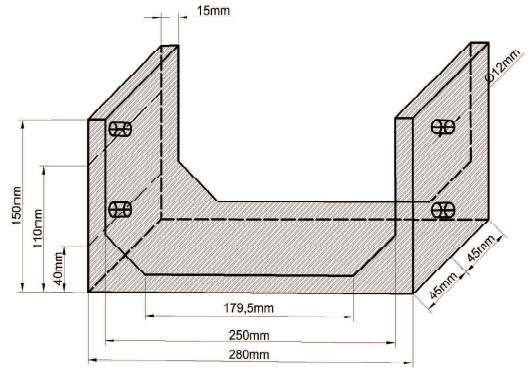

(b)

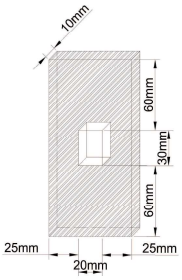

(c)

Figure 3.11: Illustration of test pieces: a) set up; b) steel apparatus; c) auxiliary metal piece x2.

tests were performed according to EN-26891 (1991). The set used for these tests is represented in figure 3.11, plus the metal pieces needed to support the timber elements so as to prevent the split during the application of the load. The side members had 60 mm of thickness and the middle member had 90 mm. In case of CLT, the laminated timber had 20 mm each in the side members and 30 mm each in the middle member.

Test procedure

At first, after all was set up, the maximum force ($F_{max,est}$) was estimated applying a monotonic force with a constant rate of 0,017 mm/s.

After knowing the maximum force, EN-26891 (1991) procedure was applied. It started with a force control applying a force until 40% of $F_{max,est}$ which was maintained for 30 seconds. Then, the force decreased at 10% of $F_{max,est}$ and maintained for 30 seconds. After that, and still in force control, the load increased until 70% of $F_{max,est}$ with a constant velocity of 20% $F_{max,est}$ (approximately). After finishing the force control, from 70% $F_{max,est}$ upwards, the displacement control was started. In this phase the velocity was maintained constant (0,017 mm/s) until 15 mm of displacement was reached.

The procedure was the same for the three types of samples (glulam, chestnut and clt). That made a total of thirty-six tests (twelve for each type). Only wood dowel was tested in order to compare it with theoretical results, as it was indicated before in this chapter. The obtained results will be presented and analysed in the following chapter (see 4).

Design formulas

On the other hand, there are design formulas that allow us to know the characteristic load-carrying capacity presented in equation 3.8.

$$F_{v,Rk} = \min \begin{cases} f_{h,1,k} t_1 d & (I) \\ 0,5 f_{h,2,k} t_2 d & (II) \\ 1,05 \frac{f_{h,1,k} t_1 d}{2+\beta} \left[\sqrt{2\beta(1+\beta) + \frac{4\beta(2+\beta) M_{y,Rk}}{f_{h,1,k} d t_1^2}} - \beta \right] + \frac{F_{ax,Rk}}{4} & (III) \\ 1,15 \sqrt{\frac{2\beta}{1+\beta}} \sqrt{2 M_{y,Rk} f_{h,1,k} d} + \frac{F_{ax,Rk}}{4} & (IV) \end{cases} \tag{3.8}$$

With:

$$\beta = \frac{f_{h,2,k}}{f_{h,1,k}} \tag{3.9}$$

Where $F_{v,Rk}$ is the characteristic load-carrying capacity per shear plane per fastener, t_i is the timber or board thickness or penetration depth, with i either 1 or 2, $f_{h,i,k}$ is the characteristic embedment strength in timber member i, d is the fastener diameter, $M_{y,Rk}$ is the characteristic fastener yield moment, β is the ratio between the embedment strength of the members, $F_{ax,Rk}$ is the characteristic axial withdrawal capacity of the fastener.

The term $F_{ax,Rk}/4$ is the contribution from the rope effect. The contribution to the load-carrying capacity due to the rope effect with dowel fastener is zero.

Corresponding failure modes should be analysed in figure 3.12.

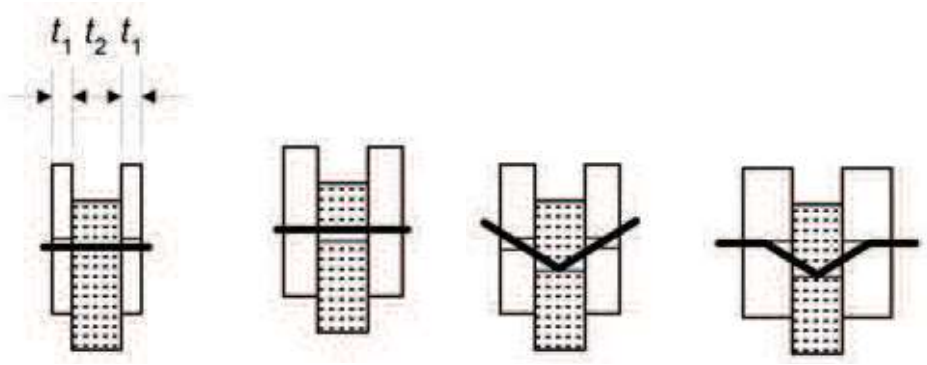

(a) (b) (c) (d)

Figure 3.12: Failure modes: a) Mode I; b) Mode II; c) Mode III; c) Mode IV (Adapted from (EN-1995-1-1, 2004)).

EN-1995-1-1 (2004) design rules were formulated exclusively for metal dowel type fasteners, which means that all variables for double shear, for example $M_{y,Rk}$, is concerned with steel dowels. Thus, some calculations will be made taking into account some equations presented in 3.3.4.

This page intentionally left blank.

Chapter 4

Results and Discussions

This chapter presents the results and the analysis of all tests performed during the development of this project. In order to verify the performance and failure mode of the different materials used, a series of tests was held to analyse the behavior of each type of wood. As known, this project aims to study the behavior of wood dowel comparatively to steel dowel. As such, the principles of EN-1995-1-1 (2004) were taken into account and then five types of experiences were chosen to verify the material behavior.

To be sure that every result is well understood it will be divided into four sections, namely: compression characterization of wood dowels; dowel-bearing strength; embedment strength of dowel type fasteners; and double shear with wood dowels.

For the brevity and organization of this chapter, only one specimen will be analysed in each section thus, the summary of all results will be presented at the end of each section.

4.1 Compression characterization of wood dowels

The main objective of the present experiment is to analyse the compression capacity of the wood used as dowel. Thus, twenty-two specimens were tested in order to know better the Massaranduba mechanical capacity to support compressive strength parallel to its fibres.

In figure 4.1 the configuration of the fifteenth sample tested are presented, before and after the application of the load. Therefore, by analysing figure 4.1(b), the failure mode is perfectly visible, and it can be called a shearing rupture. This type of rupture

means that the failure plan makes more than 45 degrees with the top of the specimen. This type of failure occurred similarly to all of the twenty-two specimens tested.

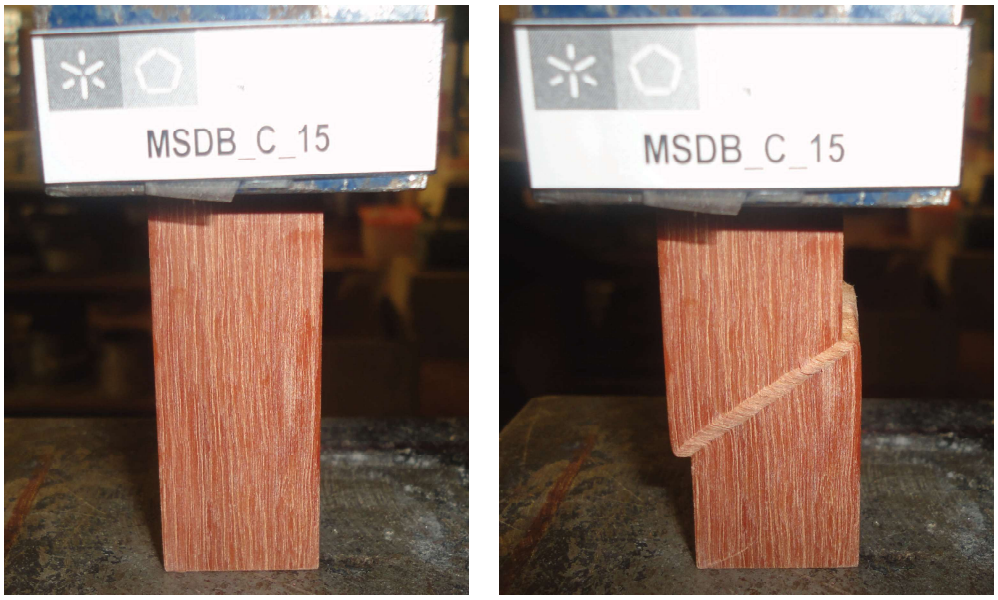

(a) (b)

Figure 4.1: Images of samples before and after the test: a) before; b) after.

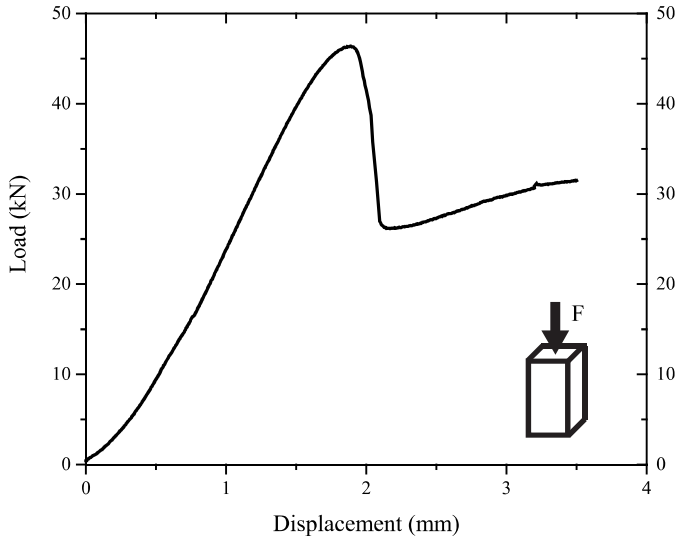

Figure 4.2: Load-Displacement curve for selected specimen.

The load-displacement curve obtained by testing the fifteenth sample is presented in figure 4.2. Analysing the curve, the sample had elastic behavior with stiffness until it reached the maximum load of 46 kN, after 3 minutes into the test, and then the

failure takes place and a post-elastic phase appears. It can also be seen that after the failure, the specimen continues to resist with some hardening which indicates that massaranduba, when loaded parallel to its fibres with a compressive load, has ductile failure.

To sum up, analysing figure 4.3 and the table 4.1 where it is presented the COV, besides other parameters, of the maximum force (1,65%) and compression strength (1,57%), which indicates low variability as well as uniformity of the results.

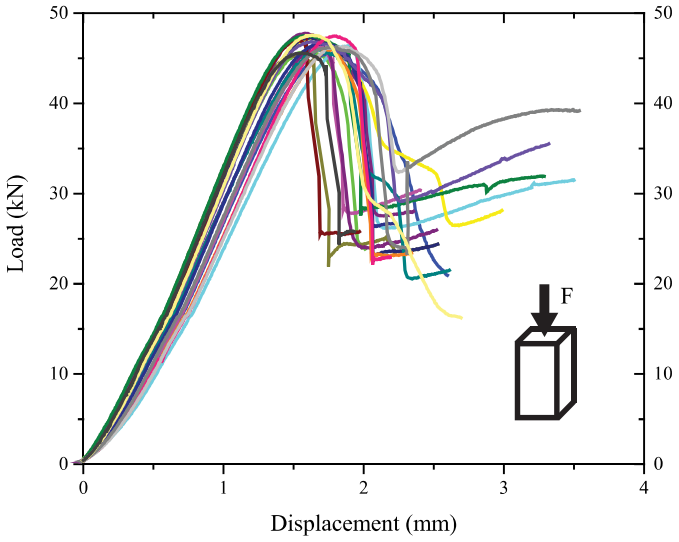

Figure 4.3: Load-Displacement curve for selected specimen.

Table 4.1 shows the compression test results obtained for each sample concerning maximum load (F_{max} in kN) and compression strength parallel to grain ($f_{c,o}$ in N/mm^2). The mean and COV (%) are also presented to show the variability of results.

4.2 Dowel-bearing strength

Twelve specimens were tested at radial compression perpendicular to dowel grain and with maximum confinement of the dowel. Images before and after the procedure are shown in figure 4.4. Only one dowel is shown. However, the failure mode occurs similarly to all specimens tested and the proof is the uniformity of the results presented in figure 4.5. By analysing data and visual deformation, it can be concluded that when subjected to maximum confinement, the massarranduba dowel has linear-elastic behavior with linear hardening and permanent deformation.

Table 4.1: Physical parameters and compressive tests results.

Sample	Dimensions (mm)	Density (kg/m^3)	F_{max} (kN)	$f_{c,o}$ (N/mm^2)
1	20,46 x 20,51 x 50	1095,72	46,94	111,54
2	20,46 x 20,41 x 50,09	1079,51	45,32	108,54
3	20,30 x 20,44 x 50,06	1084,18	45,78	110,33
4	20,46 x 20,39 x 50,06	1087,44	45,53	109,13
5	20,46 x 20,39 x 50,13	1077,79	46,43	111,30
6	20,53 x 20,51 x 50,05	1092,31	46,29	109,93
7	20,47 x 20,45 x 50,14	1073,89	47,26	112,89
8	20,49 x 20,47 x 50,09	1068,58	45,31	108,02
9	20,48 x 20,46 x 50,06	1071,22	47,31	112,90
10	20,47 x 20,45 x 50,02	1086,97	46,71	111,58
11	20,51 x 20,49 x 50,16	1081,61	47,78	113,69
12	20,48 x 20,55 x 50,17	1069,87	47,04	111,78
13	20,47 x 20,53 x 50,07	1091,99	47,51	113,06
14	20,48 x 20,53 x 50,09	1069,77	45,96	109,30
15	20,49 x 20,53 x 50,07	1103,39	46,63	110,85
16	20,45 x 20,41 x 50,05	1090,95	46,11	110,47
17	20,49 x 20,52 x 50,07	1093,00	46,84	111,42
18	20,43 x 20,55 x 50,10	1087,30	47,50	113,13
19	20,45 x 20,49 x 50,11	1069,67	46,28	110,44
20	20,47 x 20,51 x 50,11	1088,23	46,26	110,19
21	20,49 x 20,46 x 50,19	1063,17	47,59	113,53
22	20,56 x 20,51 x 50,02	1081,42	45,59	108,11
	Mean	1082,17	46,54	111,02
	COV (%)	0,98	1,65	1,57

(a) (b)

Figure 4.4: Images of samples before and after the procedure. a) Before. b) After.

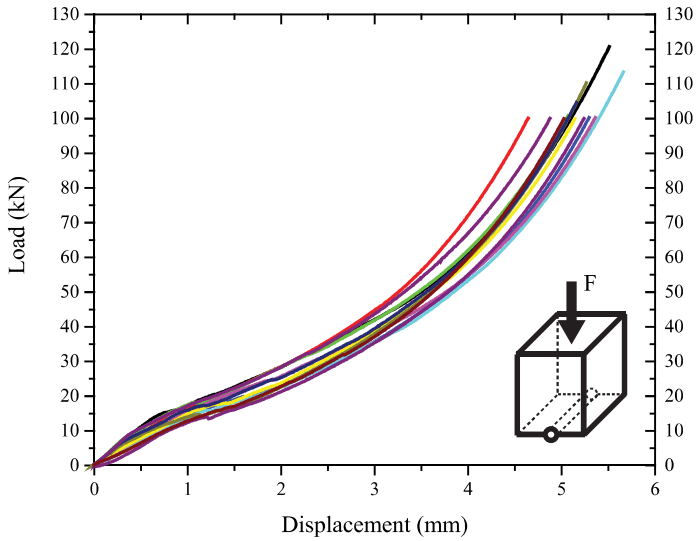

Figure 4.5: Load-displacement curves obtained in dowel-bearing tests

4.3 Embedment strength of dowel type fasteners

It is important to note that the present experiment was divided into two phases, namely, wood dowels and steel dowels and also, for each type of fastener, three different types of wood members were tested. As such, the results will be analysed in three phases to ensure that the obtained results are well understood. Therefore, the following subsections will be divided in wood dowel results, steel dowel results and finally a comparison between them. At the end, another comparison will be presented but in this case will be between glulam, chestnut and CLT.

4.3.1 Wood dowel

This subsection will also be divided into other three, this way the discussion becomes more pleasant to readers.

It is important to report that all embedment tests procedures started with a preload of 0,2 kN.

4.3.1.1 Glulam

First two monotonic tests were performed in order to predict the maximum load (see figure 4.6(a)), after that the parameters were defined in accordance with the

standard principles.

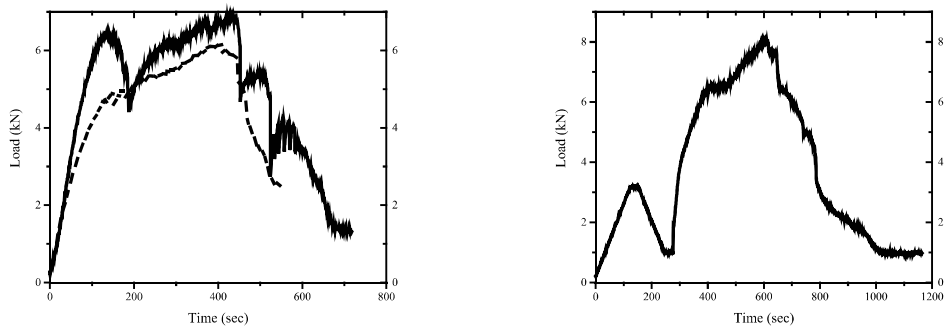

(a) (b)

Figure 4.6: Load-time curves for glulam: a) monotonic tests; b) embedment tests procedure.

The solid line corresponds to the first monotonic test, while the dash line represents the second monotonic test were the rate was adjusted to 0,017 mm/s so that the load should reach its maximum within (300 ± 120) seconds. Thus, the parameters for the remain samples were set and the analysis should be made taking into account the figure 4.6(b) were procedure adopted is presented.

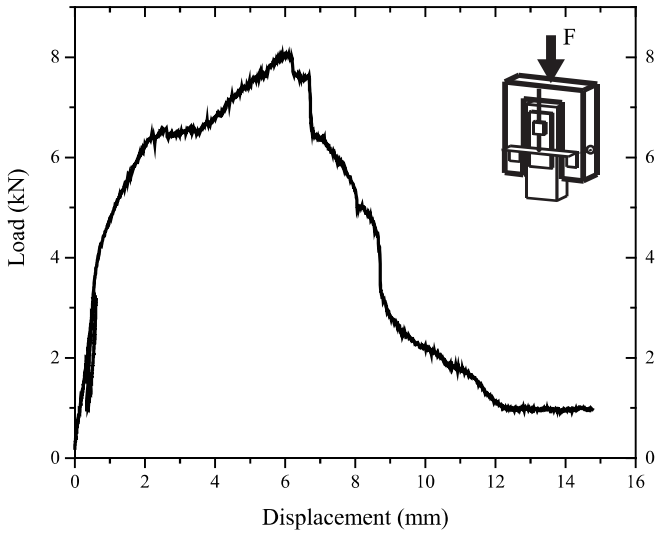

Figure 4.7: Load-displacement curve for selected sample.

Therefore, the procedure was divided into two phases, force control and displacement control, respectively. In the first phase, the test was executed with constant rate

of 0,021 kN/s; the load was applied until 2,75 kN (which comes from 40% of $F_{max,est}$ obtained in the second monotonic test) and maintained for 30 seconds. After that, the load increased until 0,69 kN (10% of $F_{max,est}$) and then maintained for 30 seconds. The second phase took place and the load started to increase with constant rate (0,017 mm/s) until the maximum load was reached or until 15 mm of displacement.

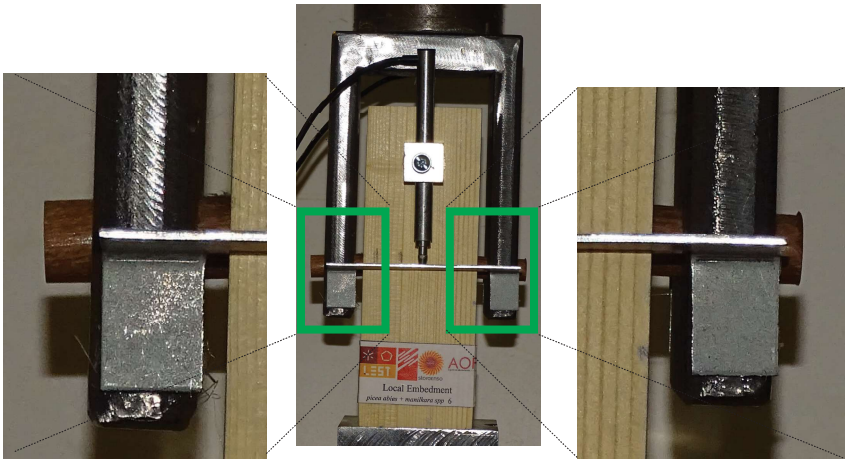

(a)

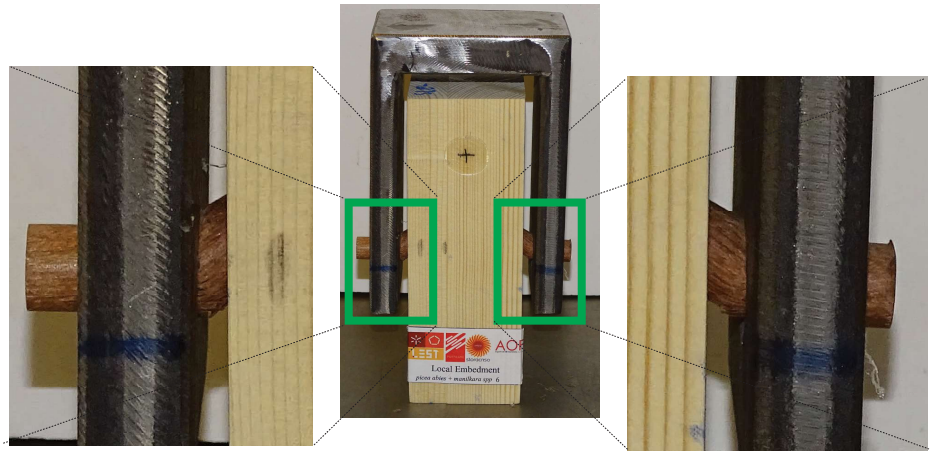

(b)

Figure 4.8: Details of selected specimen before and after the procedure: a) before; b) after.

Figure 4.7 presents the result for some glulam specimen randomly chosen to be analysed. The figure starts with a linear phase that is interrupted by a yield level where the displacement occurs to constant load, mostly due to the interference of dowel. Afterwards, the sample continues to resist to the applied load until the maximum load is reached. Then the failure occurs and the capacity to resist the applied load started to decrease. When the sample attained 12 mm of deformation it can be seen that the

material had the capacity to continue to deform at a constant load for some time. This means that glulam member with massaranduba dowel has ductile rupture.

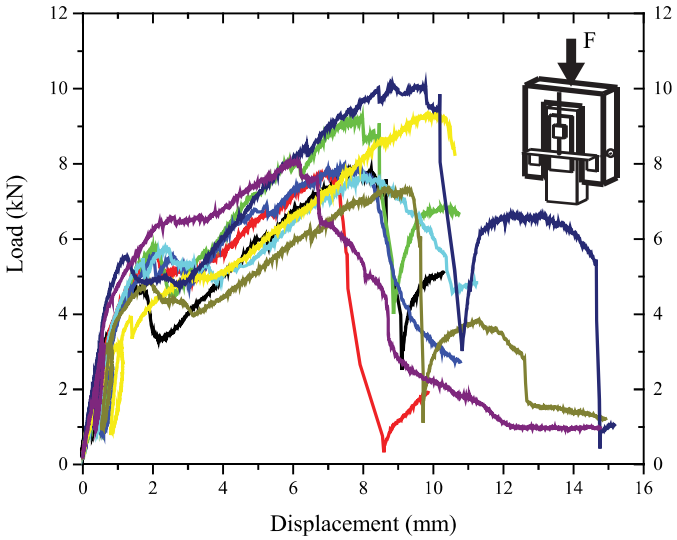

Figure 4.9: Spruce force-displacement results.

Figure 4.8 and figure 4.10 shows the specimen before and after being tested were the deformation of the element and dowel can be analysed from front side and element cross section. The dowel needs to be cut in order to enable the disassembly of that set up and start a new one. See also figure 4.9 where the general behaviour and the low variability of the results can be analysed.

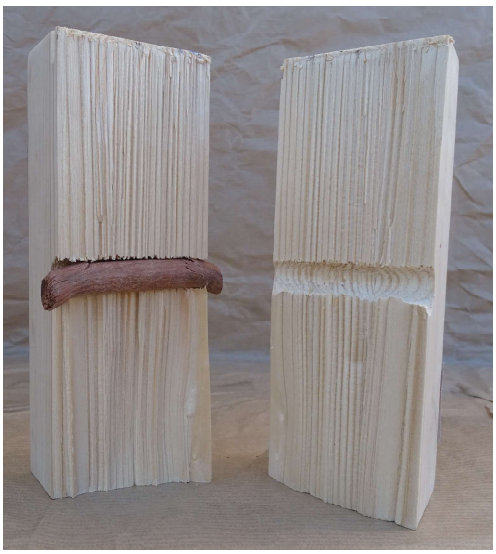

Figure 4.10: Cross section.

4.3.1.2 Chestnut

To start, one monotonic test with constant rate of 0,017 mm/s was performed (see figure 4.11(a)) to get to know the estimated force. The maximum force reached by sample number one was 11,74 kN. Therefore, to explain figure 4.11(b), the procedure set for samples started with force control with a constant rate of 0,039 kN/s until, 4,70 kN (40% of $F_{max,est}$) and stays there for 30 seconds. Then, the load decreased with the same rate (0,039 kN/s) and stays for 30 seconds at 1,17 kN/s (10% of $F_{max,est}$). After that procedure, the displacement control started where the maximum load of samples was reached with a constant velocity of 0,017 mm/s.

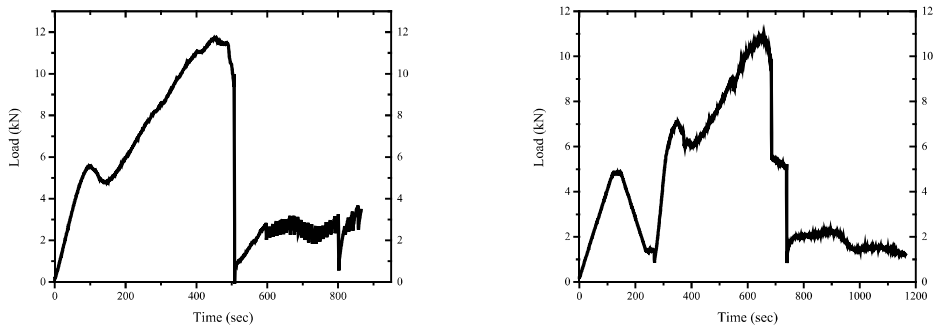

(a) (b)

Figure 4.11: Load-time curves for chestnut: a) monotonic test; b) embedment tests procedure.

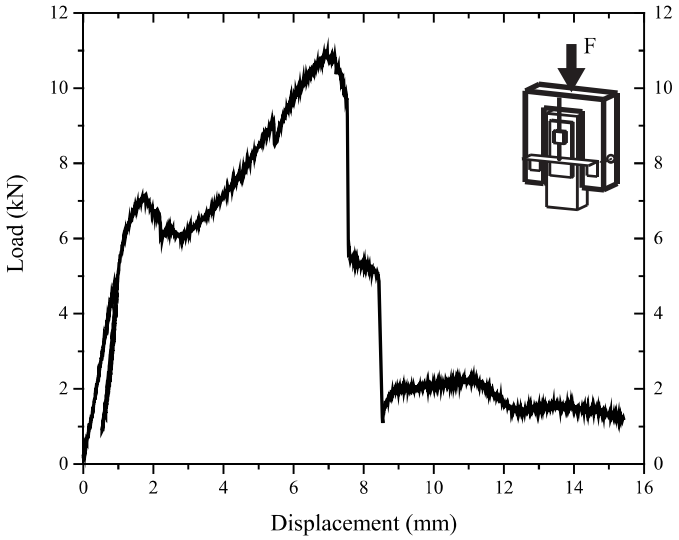

Figure 4.12: Load-displacement curve for selected sample.

Analysing figure 4.12, the elastic limit happens with 2 mm of displacement after which a slight yield level with deformation at a constant load appears. Then the element continued to resist the applied load until the maximum load was attained and the failure occurred. In this case, some load-carrying capacity is also present even after the set failure achieving the ductile failure as desirable.

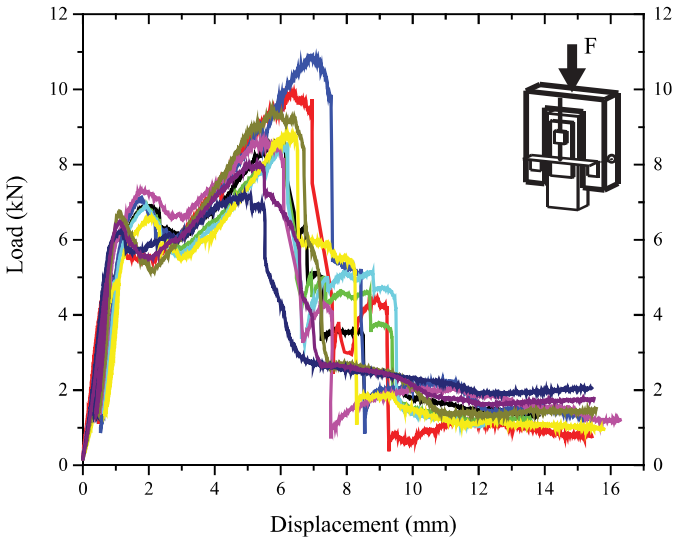

Figure 4.13: Load-displacement curves for all specimens tested.

The physical conditions before and after the test are presented in figure 4.14 and 4.15 were the failure mode of the specimen is perfectly visible. All specimens deformed similarly to the one presented below.

Figure 4.14: Cross section.

It is also important to report the results of all specimens so that the behaviour of all series of tests can be analysed. Therefore, some variability of the results can be noticed concerning the maximum force reached (COV of 13,84%) which was predicted due to, for example, the anisotropy of the material and the dowel confinement, although in all specimens the ductile failure was visible.

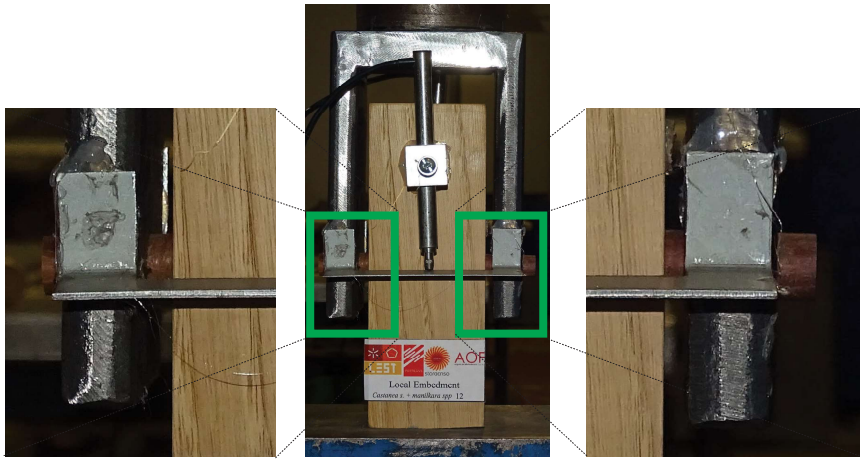

(a)

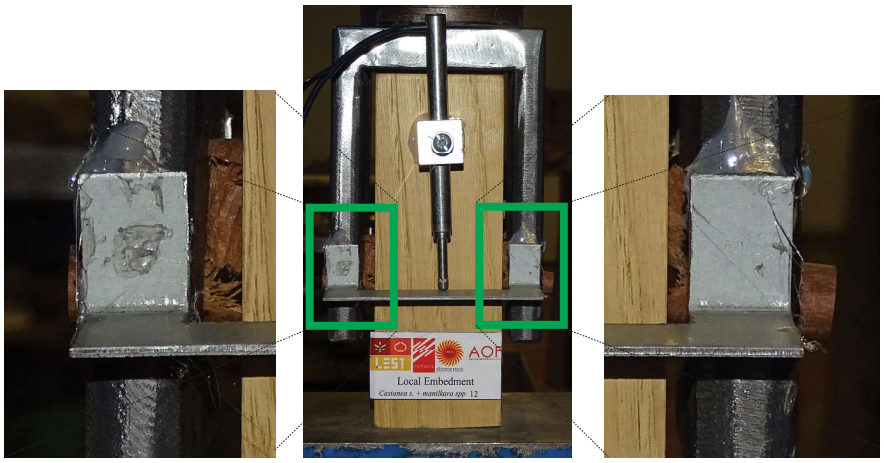

(b)

Figure 4.15: Chestnut images before and after testing: a) before. b) after.

4.3.1.3 CLT

For cross laminated timber tests with massaranduba dowel the procedure was the same as glulam and chestnut. First, a monotonic test was performed (see figure 4.16(a)) to predict the maximum force ($F_{max,est}$) and then the procedure for the remain specimens was set. Thus, figure 4.16(b) presents the adopted procedure were in the first phase the load increased until 3,54 kN (40% of 8,86 kN) with constant rate of 0,03 kN/s

and maintained there during 30 seconds. Then the load started to decrease with the same rate as before and stayed at a constant load of 0,89 kN (10% of 8,86 kN) about 30 seconds. The displacement control started, after those 30 seconds, with 0,017 mm/s, until the maximum force was reached. To better understand the elements behavior, the test stopped only when 15 mm of deformation was achieved (see figure 4.16(b)).

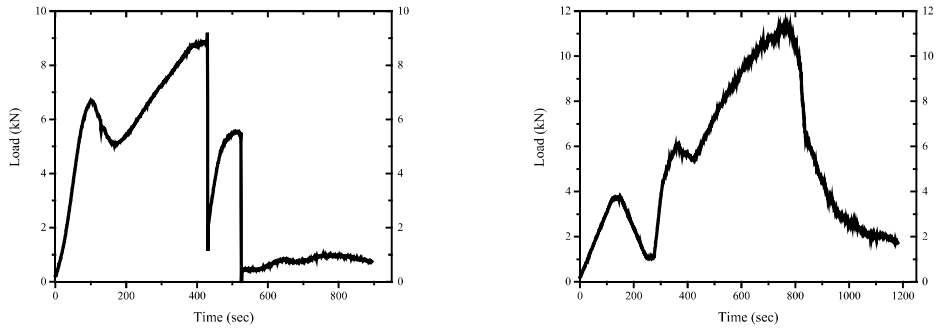

(a) (b)

Figure 4.16: Load-time curves for CLT: a) monotonic test; b) embedment tests procedure.

In figure 4.17 it is shown the behavior of a CLT sample where it can be noticed, once again, ductile rupture.

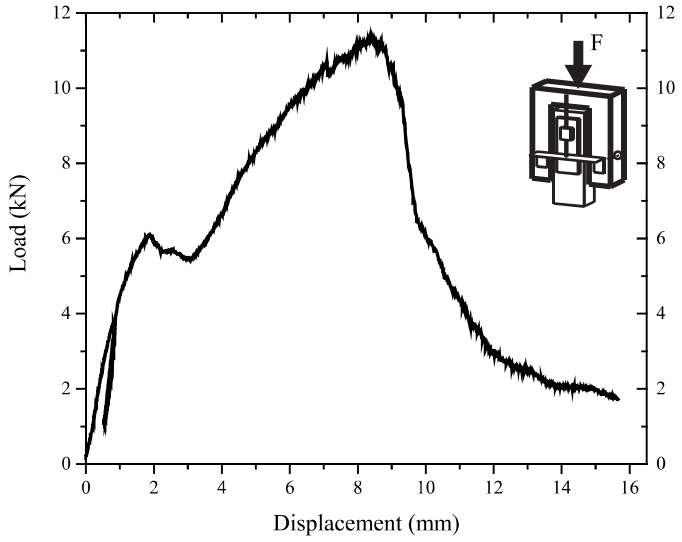

Figure 4.17: Load-displacement curve for selected sample.

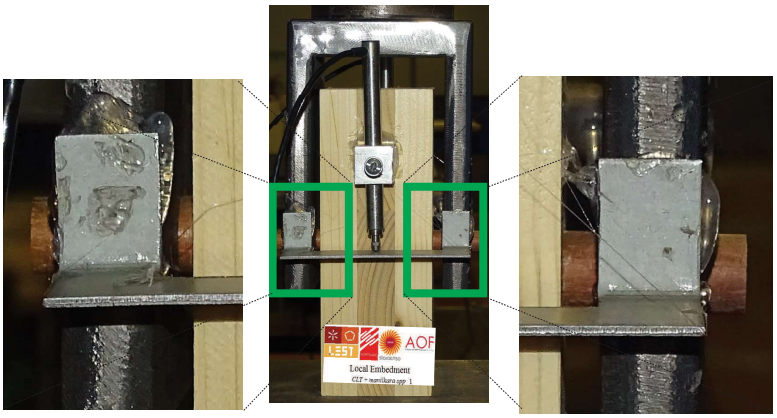

(a)

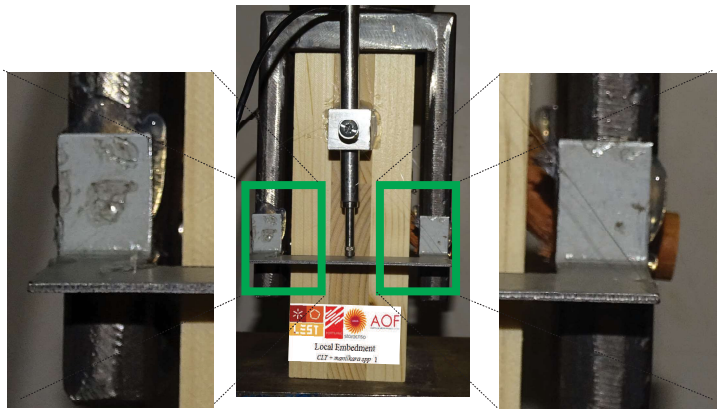

(b)

Figure 4.18: CLT images before and after testing: a) before; b) after.

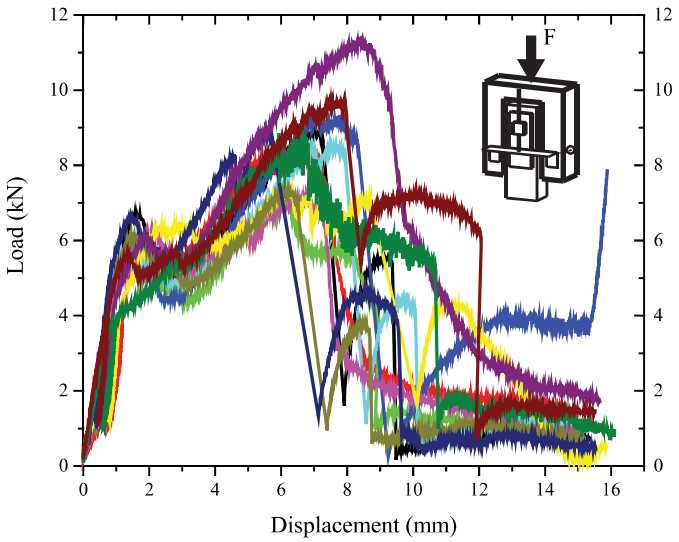

Figure 4.19: CLT force-displacement results.

After the elastic yield, the set started to resist the applied load until the maximum load is reached and the failure happens. After the load-peak a smooth decrease of load-carrying capacity is noticed, mostly due to dowel lost of resistance. What was said can be proven with figure 4.18 in which the visual failure is presented.

To sum up, the global behavior is shown in figure 4.19 where the variability of the results is presented mostly due to the timber physical conditions.

4.3.2 Steel dowel

4.3.2.1 Glulam

Figure 4.20(a) presents the monotonic results which were considered to set the embedment tests procedure.

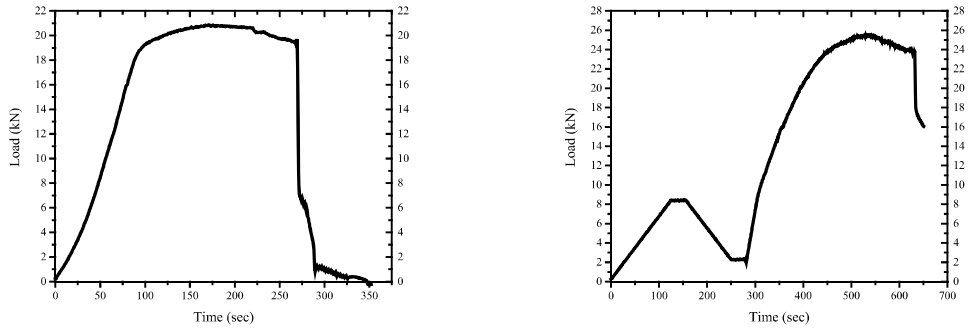

(a) (b)

Figure 4.20: Load-time curves for glulam element with steel dowel: a) monotonic test; b) procedure.

Thereby, figure 4.20(b) represents the adopted procedure with initial load at constant rate (0,07 kN/s) until 8,34 kN (40% of 20,86 kN) and maintained for 30 seconds. Then the applied load decreased at 2,09 kN (10% of 20,86 kN) and was maintained for 30 seconds. From this phase until the end of the experiment, the control was made by means of displacement with 0,017 mm/s until the maximum load was reached or until 15 mm of deformation, when feasible.

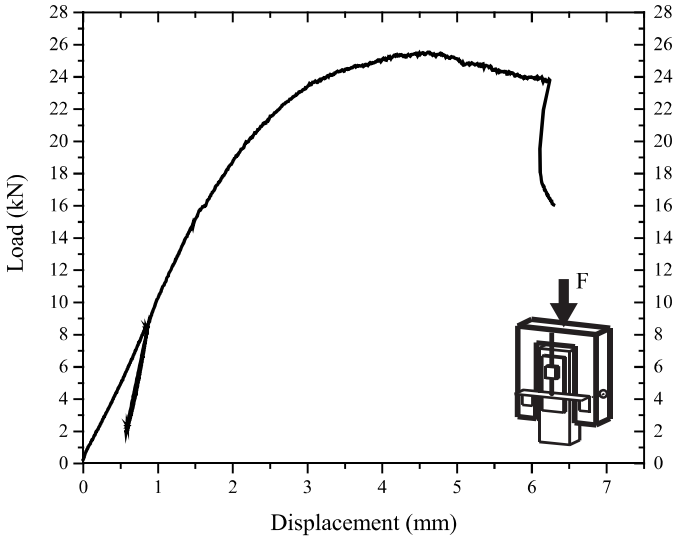

Figure 4.21: Load-displacement curves for selected specimen.

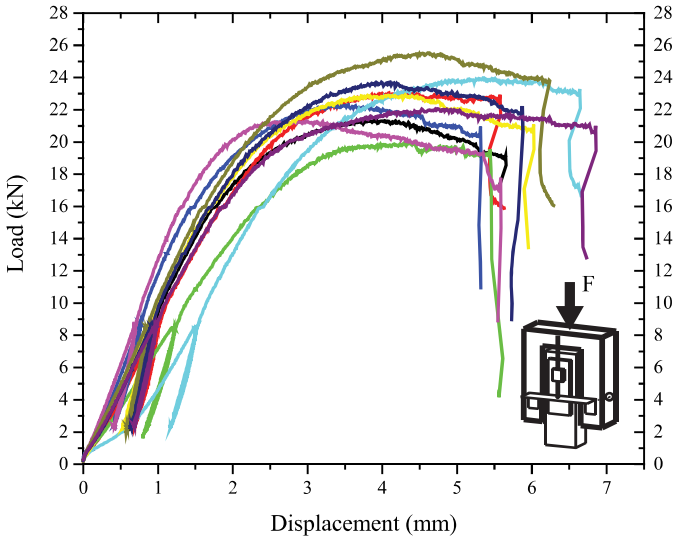

Figure 4.22: Load-displacement curves for all specimens.

Load-displacement curve for some randomly chosen specimens is represented in figure 4.21. Analysing it, after the load peak is achieved, the load carrying capacity started to decrease with low variability until that the maximum capacity of the wood member was used, provoking the element failure. In addition, it was visible during the experiment that the dowel trespassed slowly the wood member after the maximum force was reached, which is the proof of the failure noticed in the figure.

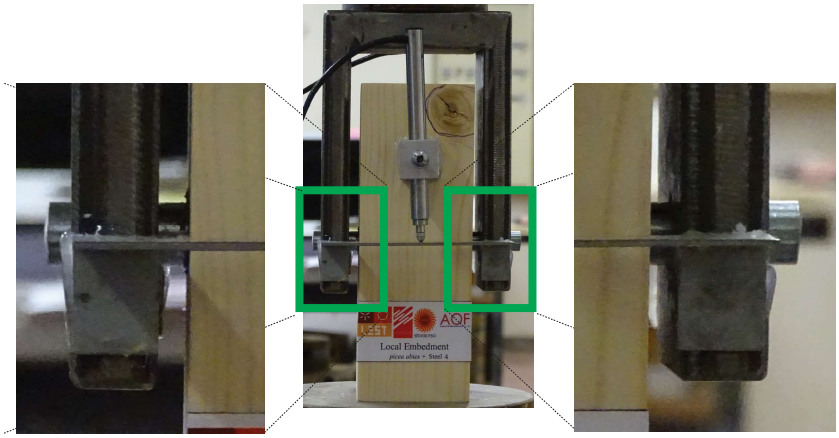

(a)

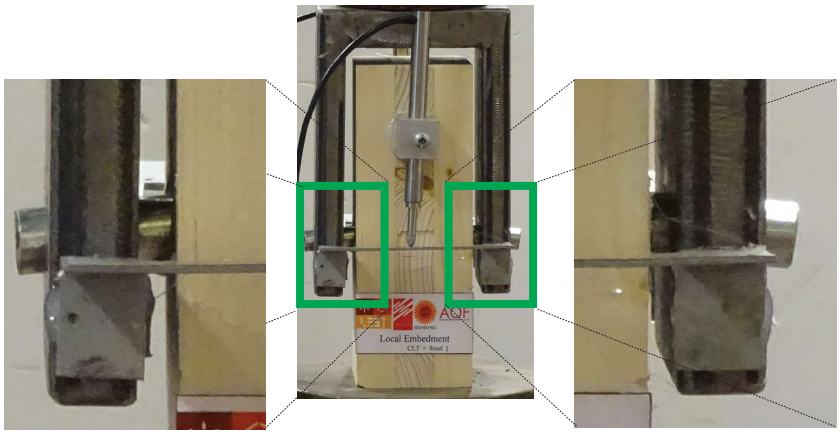

(b)

Figure 4.23: CLT images before and after testing with steel dowel: a) before; b) after.

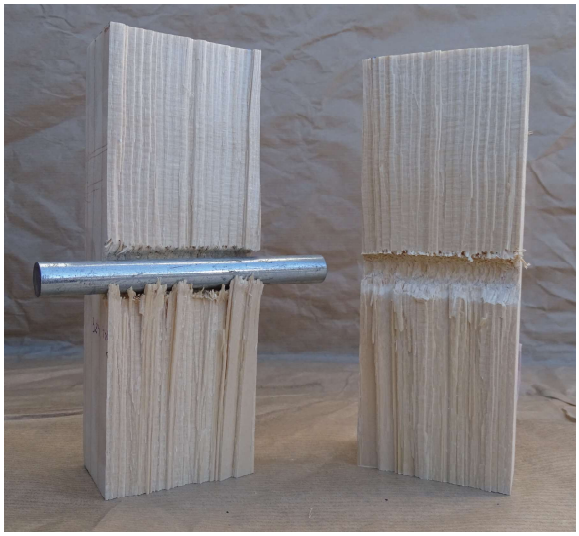

Figure 4.24: Cross section.

To sum up, in figure 4.23 and 4.24 is presented the physical failure mode of one sample tested and in figure 4.22 the load-displacement curves for all series of glulam with steel dowel tests, showing the uniformity of the results, meaning that all specimens tested failed abruptly without taking advantage of the full capacity of the dowel.

4.3.2.2 Chestnut

The monotonic test (see 4.25(a)) achieved 44,24 kN of maximum load, thereby, the procedure seen in 4.25(b) was established. This way, the load increased until 17,69 kN (40% F_{max}) and maintained for 30 seconds, then it decreased until 4,42 kN (10% F_{max}) and also maintained for 30 seconds with constant load.

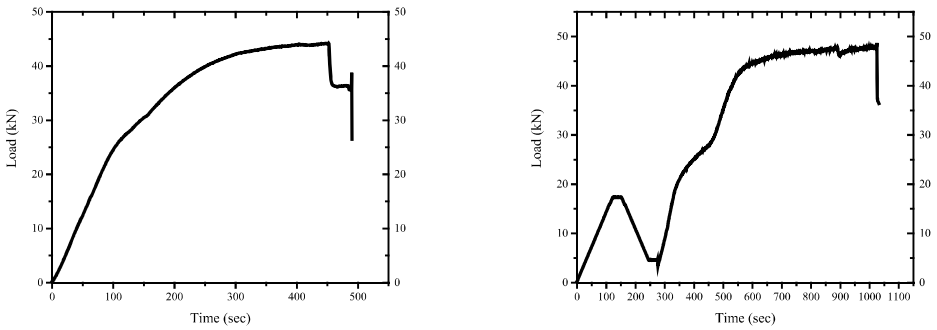

(a) (b)

Figure 4.25: Load-time curves for chestnut element with steel dowel: a) monotonic test; b) procedure.

After that the displacement started with a rate of 0,017 mm/s until the maximum load was reached. In this case, it was not possible to continue the test until 15 mm of displacement due to the total rupture of the set which occurred before that. The procedure started with a force control and constant velocity of 0,15 kN/s.

According to figure 4.26, it was noticed that after the specimen achieved the maximum load, a sudden collapse occurred that justifies the abrupt fall in the figure. The fully load-carrying capacity of the wood member was used, which did not happen with the dowel.

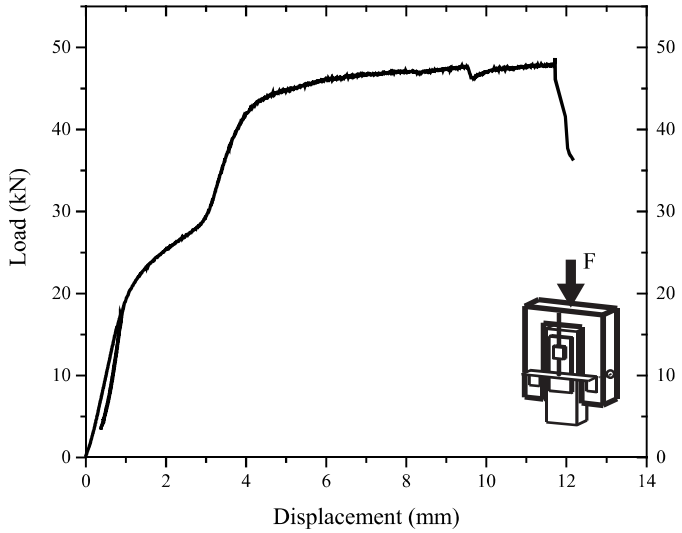

Figure 4.26: Load-displacement curve for selected sample.

Moreover, the behavior described above for the selected sample can be taken into account when analysing the global behavior, according to what is presented in figure 4.27. All specimens tested suddenly lost load-carrying capacity which resulted in, less desirable, brittle failure of the set. In addition, 4.28 and 4.29 shows the failure mode in front side view and cross section.

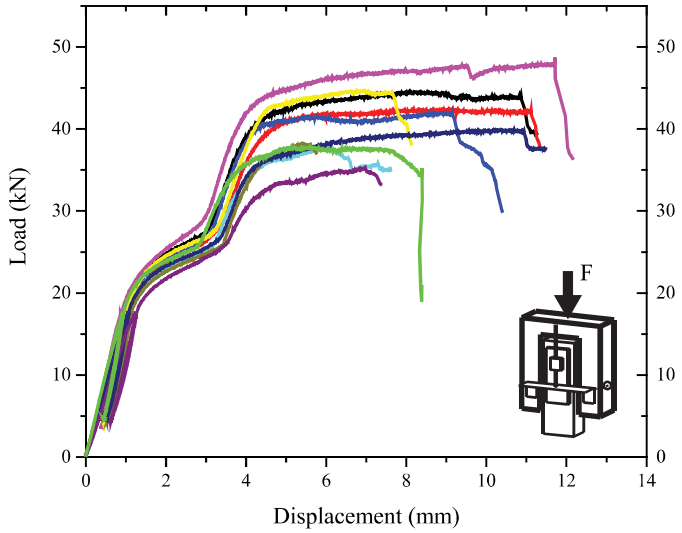

Figure 4.27: Load-displacement curve for all specimens.

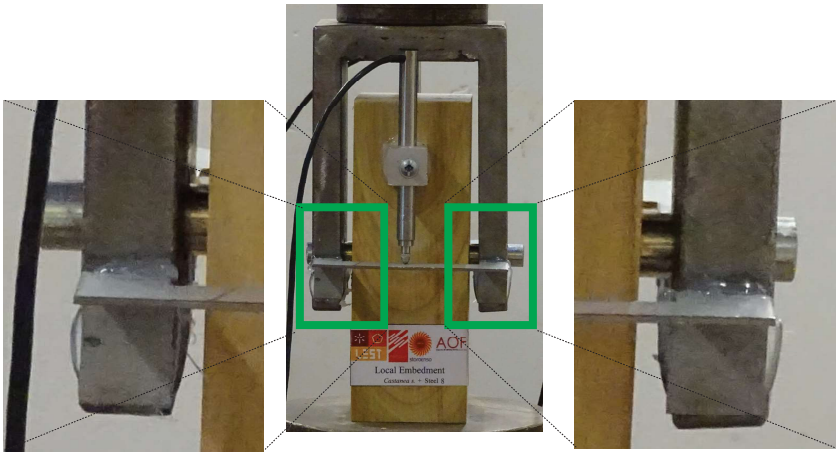

(a)

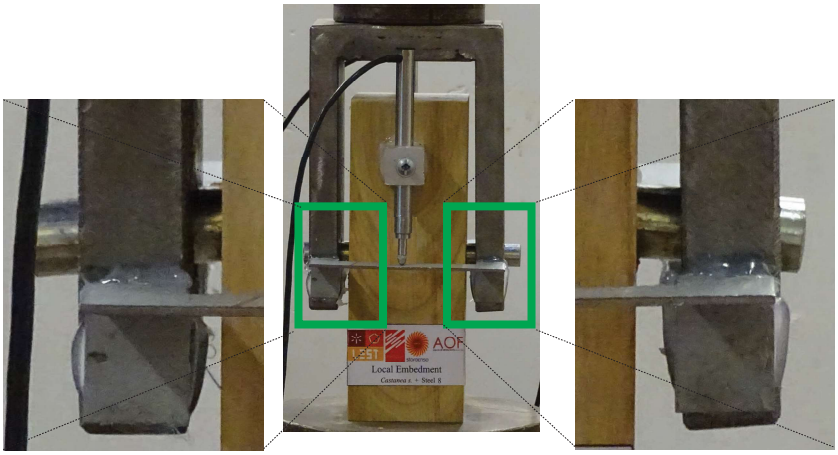

(b)

Figure 4.28: CLT images before and after testing with steel dowel: a) before; b) after.

Figure 4.29: Cross section.

4.3.2.3 CLT

This tested series was also lead by the monotonic tests that achieved 25,87 kN (see figure 4.30(a)). Thus, the remain specimens were tested according to the procedure represented in figure 4.30(b).

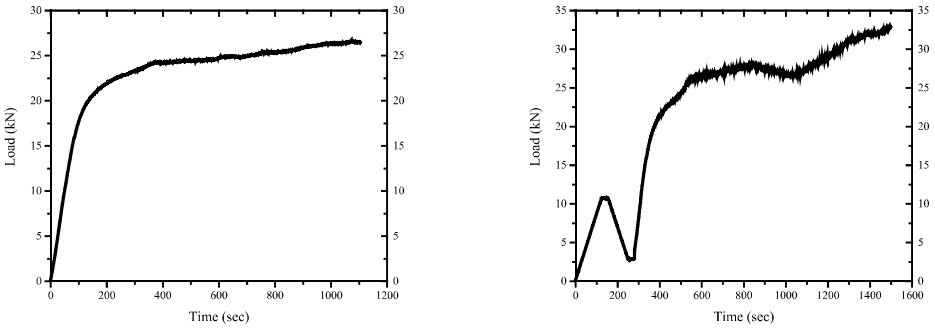

(a) (b)

Figure 4.30: Load-time curves for CLT element with steel dowel: a) monotonic test; b) procedure.

The load increased until 10,35 kN (40% F_{max}) and after maintaining for 30 seconds the load decreased until 2,59 kN (10% F_{max}) and maintained for 30 seconds. This procedure occurred in force control with a velocity of 0,089 kN/s. After this, the displacement control started until the maximum load was reached or 15 mm of displacement. In this case, in the monotonic test a permanent hardening was noticed and because of that the test stopped at 15 mm of displacement.

While analysing the load-displacement curve for one specimen it was decided not to stop the test when the 15 mm of deformation was achieved in order to better understand CLT behavior. It was noticed that the element had the capacity to endure the embedment provoked by the steel dowel with permanent hardening mostly due to the cross layer in the timber member. In fact, because this layer was loaded perpendicularly to the grain, it added resistance to the set and restrained the element to split as happened in glulam and chestnut. Instead, the middle layer was crushed by the steel dowel.

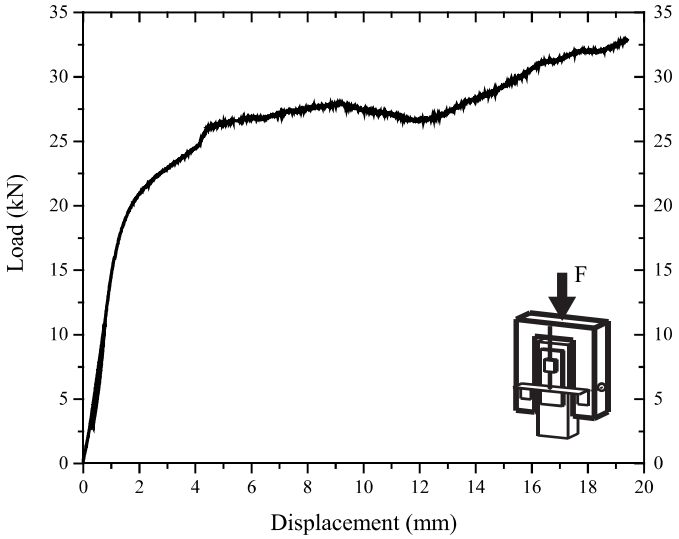

Figure 4.31: Load-displacement curve for selected specimen.

All specimens experienced continuous hardening that is evidenced by physical deformation shown in figure 4.33. In it, the external and internal member crush provoked by steel dowel which also suffered some deformation is perfectly visible. To sum up, the global results are presented in figure 4.32 that represents the load-displacement curves, in which, a pleasant uniformity of the results is visible.

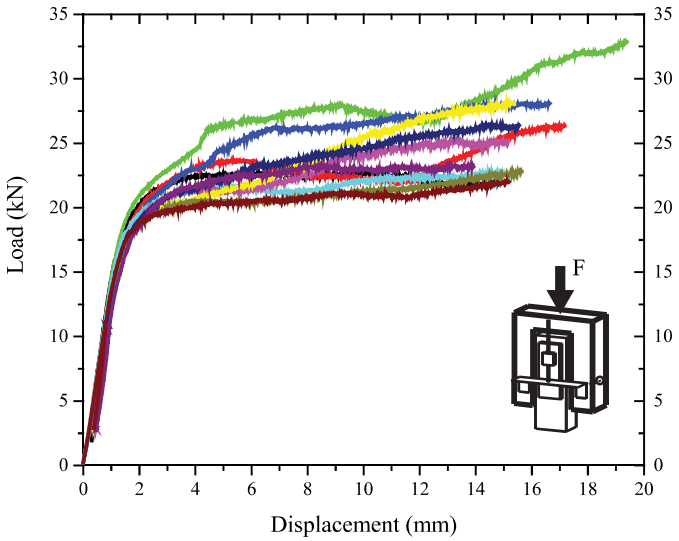

Figure 4.32: Load-displacement curves for all specimens.

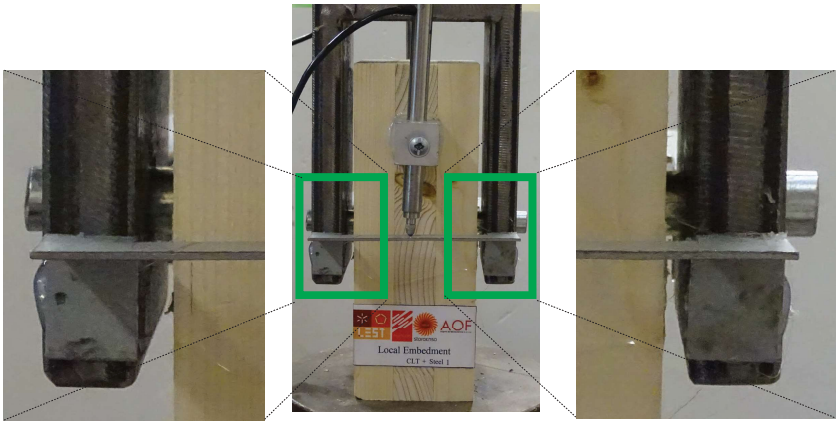

(a)

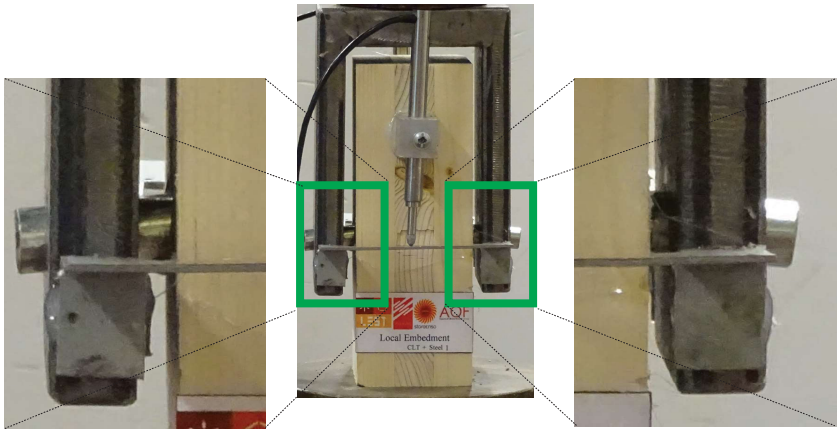

(b)

Figure 4.33: CLT images before and after testing with steel dowel: a) before; b) after.

4.3.3 Comparison between wood and steel dowels: experimental and analytical results

In order to compare the timber embedment with wood dowel or steel dowel three images are shown concerning the load-displacement curves for specimens analysed just above. Figure 4.34(a) is concerned to the difference between dowels types with glulam members, figure 4.34(b) refers to chestnut member, and 4.34(c) presents the CLT behavior. The main difference noted is the maximum load achieved by steel dowel that is higher in the three wood members. However, in glulam and chestnut with steel dowel, the failure occurred in a brittle and undesirable way unlike the wood dowel that presented ductile failure. Looking at CLT with steel dowel it is visible that after some loss of resistance, the load carrying capacity suddenly increased with hardening, due to the embedment of the cross layer in the middle. On the other hand, wood dowel does not take full advantage of the resistance capacity of CLT. However, a pleasant behavior was noted due to some plasticity of the dowel preventing brittle failure.

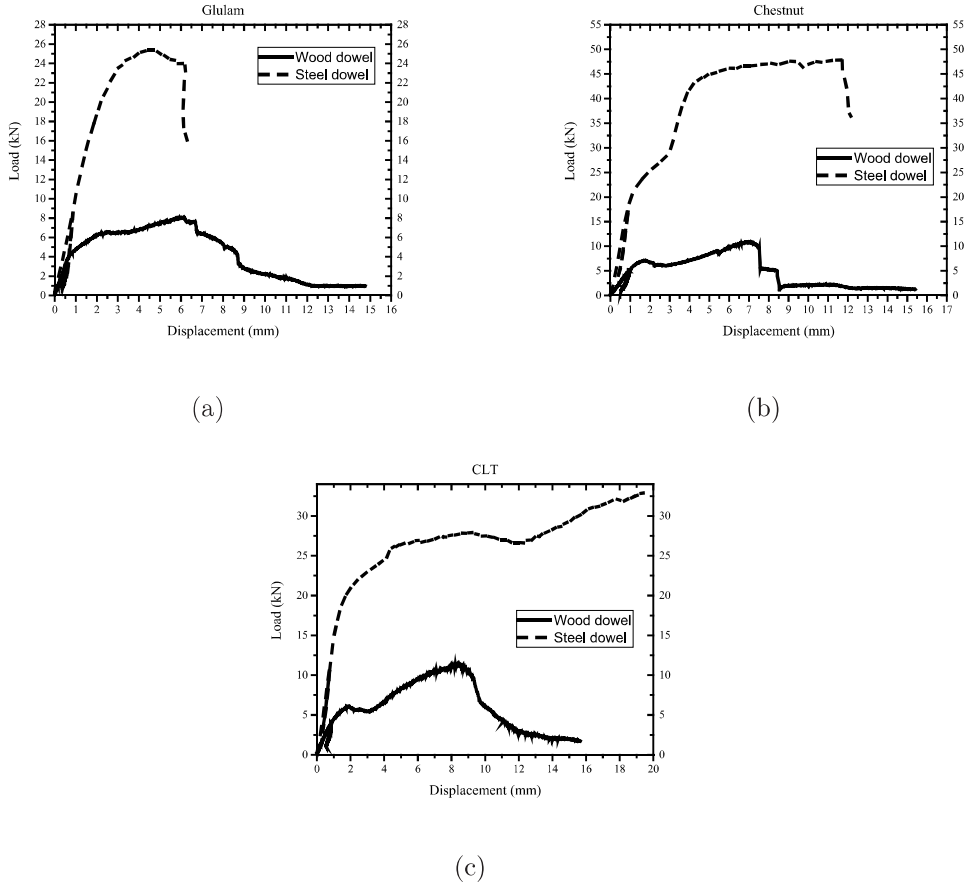

Figure 4.34: Load-displacement curves comparing wood and steel dowels: a) glulam; b) chestnut; c) CLT.

Table 4.2: Mean values for embedment strength and maximum load.

Sample	Dowel	F_{max} (kN)	$f_{h,0}$ (N/mm^2) (experimental results)	COV (%)	$f_{h,0}$ (N/mm^2) (theoretical results)
Glulam	Wood	8,16	11,33	13,93	27,42
	Steel	22,51	31,26	7,18	
Chestnut	Wood	9,14	12,70	13,61	50,51
	Steel	41,45	57,56	8,89	
CLT	Wood	8,61	11,96	14,60	30,31
	Steel	25,20	35,01	9,43	

In table 4.2 are quoted the mean values for F_max and f_h for each material variable

studied and the design values according to EN-1995-1-1 (2004). Steel dowel experienced lower variability of the results. However, the failure mode of the timber member was less desirable than with wood dowel, except for CLT. In terms of force quantification, chestnut had higher values mostly due to its density and average hardness compared with Norway spruce used for glulam and CLT. The embedment strength results are calculated by means of experimental results, according to equation 3.2 or by design rules, that assume dowels as being made only with steel, using the equation 3.3. For all calculations mean values were used instead of characteristic ones. Density mean values are quoted in Chapter 3 according to material strength class and European graded standards.

In terms of comparison between experimental an theoretical results, the overestimation of the design rules concerning wood fasteners can be put into evidence.

4.3.4 Yield moment

In figure 4.35 are presented the load-displacement curves for bending tests of wood dowels. After achieving the maximum load, the dowel started to fail gradually by means of one central hinge, between the applied load. Physical conditions before and after the tests are shown in figure 4.36

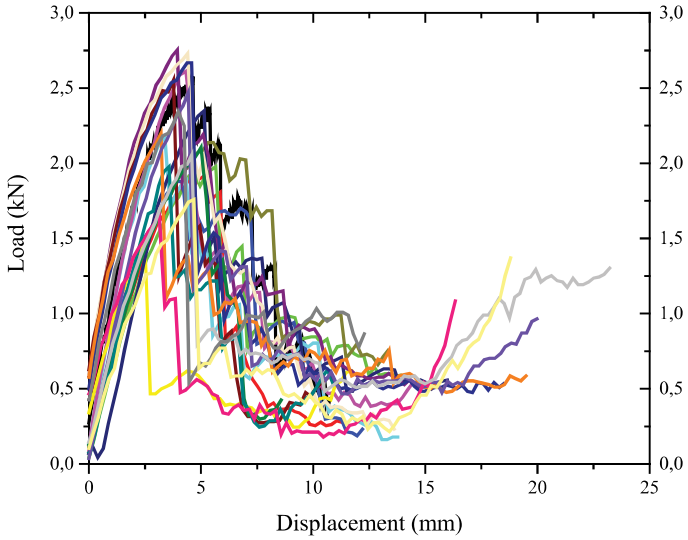

Figure 4.35: Load-displacement curves for massaranduba dowel type fasteners.

The mean value for F_{max} was 2,21 kN. It was adopted $F_{max}/2$ for F_1 and F_3 since there was no way to know the exact values with the set up adopted. Therefore, taking

into account the results and the set up dimensions described in Chapter 3, section 4.3.4, the mean value of M_y (yield moment of the dowel) is 44,17 kN.mm with 16,50% of COV. The analytical yield moment given by equations 3.6 and 3.7 is 0,464 kN.mm.

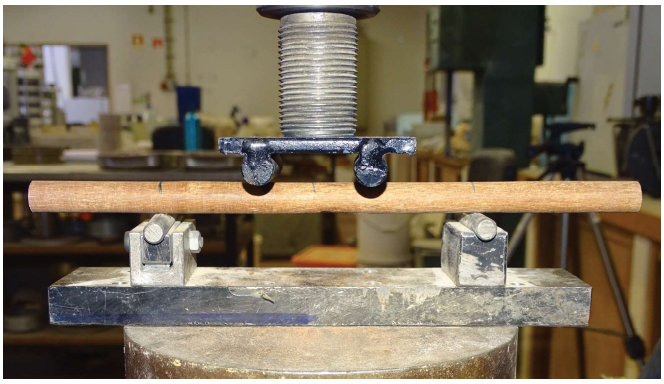

(a)

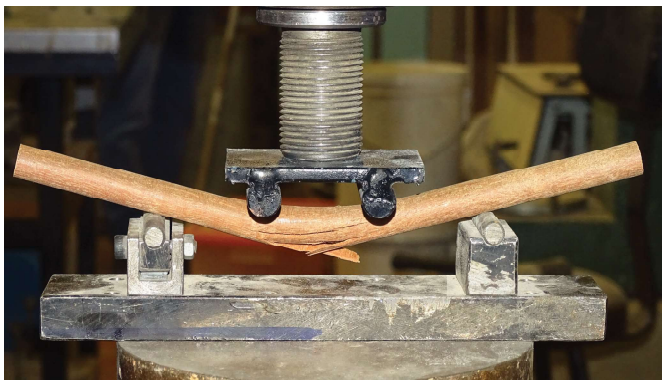

(b)

Figure 4.36: Massaranduba dowels before and after the bending test: a) before; b) after.

4.4 Double Shear with wood dowels

This section will be divided into two subsequent sections namely, experimental results and comparison between the experimental and theoretical results.

4.4.1 Experimental results

This will also be divided by type of wood for a better understanding of the results.

4.4.1.1 Glulam

Initially a monotonic test was performed to obtain the maximum load estimated. The procedure in figure 4.37(b) is a consequence of that result. Thus, the load increased in force control at a rate of 0,038 kN/s until 4,43 (40% F_{max}) and maintained for 30 seconds. Then the load decreased until 1,11 (10% of F_{max}), maintained constant for 30 seconds and then decreased until 70% of F_{max} after which the displacement control began and the maximum load achieved (see figure 4.37(b)).

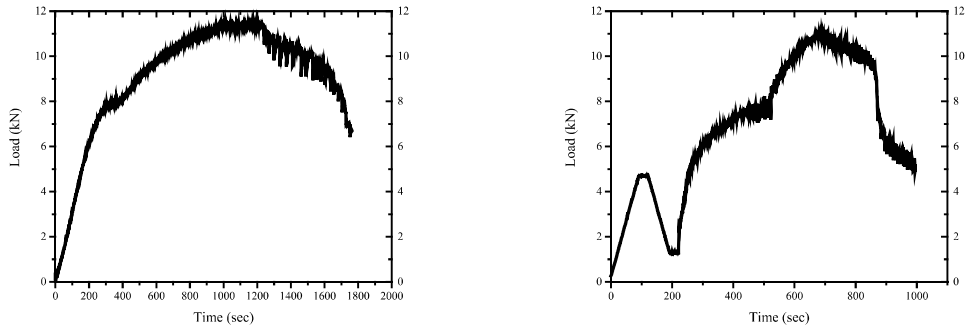

(a) (b)

Figure 4.37: Load-time curves: a) monotonic test; b) procedure.

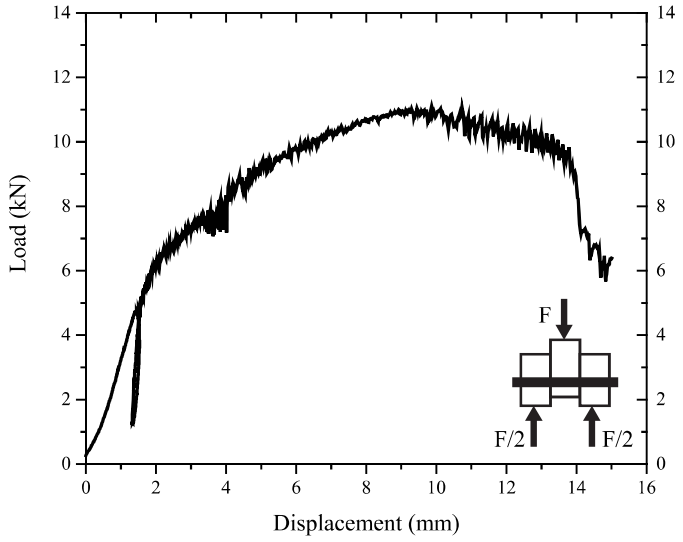

Figure 4.38: Load-displacement curve for selected specimen.

(a)

(b)

(c)

Figure 4.39: Glulam images before and after testing in double shear: a) before; b) after; c) cross section.

The load-displacement curve regarding the procedure described above is presented in figure 4.38, where the behavior of the specimen can be analysed. Therefore, the specimen experienced linear-elastic behavior after which the load-carrying capacity started to increase smoothly until its maximum. The dowel failure started to appear and the set resistance decreased as a consequence.

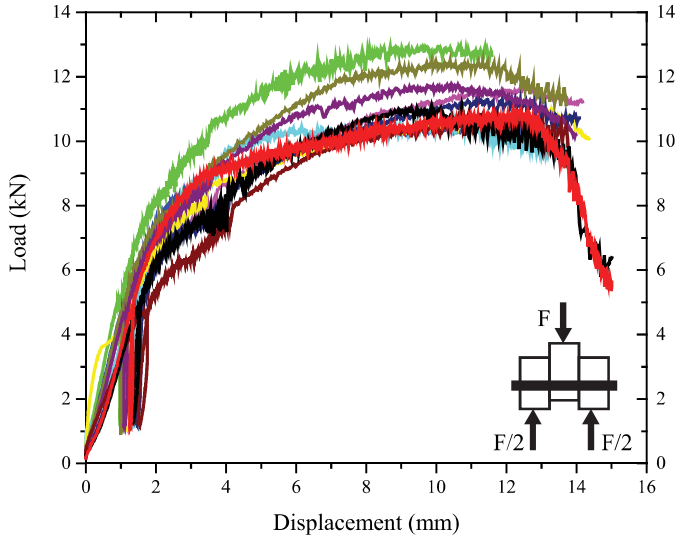

Figure 4.40: Load-displacement curve for all specimens.

The physical conditions of the side members and dowel are shown in figure 4.39. As it can be seen, the failure mode of the joint is, according to (EN-1995-1-1, 2004), mode IV in which two plastic hinges are formed.

4.4.1.2 Chestnut

Monotonic test and double shear tests procedure for chestnut in double shear are presented in figure 4.41. The maximum load achieved in monotonic test was 13,1 kN with which 40%, 10% and 70% of F_{max} was found and the rate for force control also calculated.

The joint experienced at first a linear-elastic behavior and then in displacement control the maximum load was achieved. The dowel capacity started to decrease after the load peak which explains the load fall in figure 4.43.

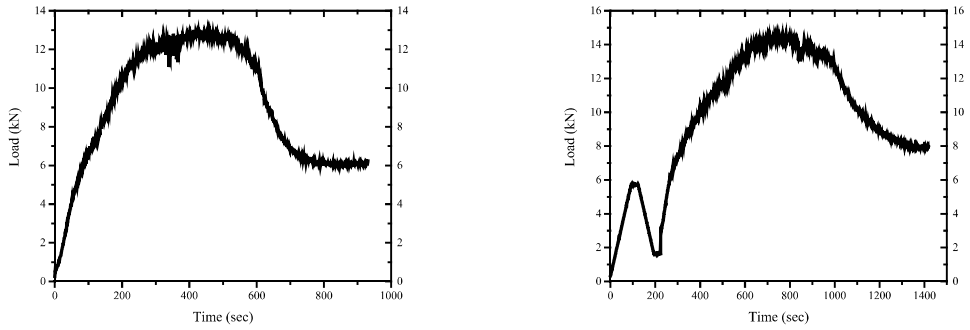

(a) (b)

Figure 4.41: Load-time curves: a) monotonic test; b) procedure.

(a)

(b)

Figure 4.42: Chestnut images before and after testing in double shear: a) before; b) after.

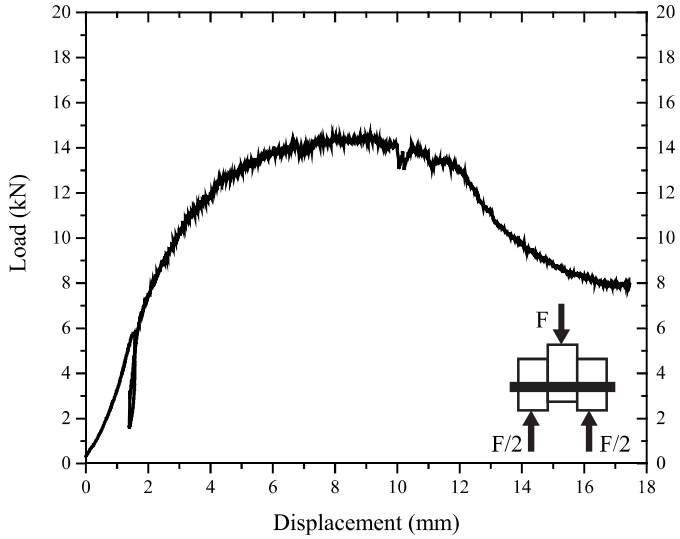

Figure 4.43: Load-displacement curve for selected specimen.

Therefore, figure 4.42 presents the physical conditions of one specimen tested, before and after the deformation. In 4.45 the desirable plastic hinges of the dowel can be seen after testing the joint. The failure mode corresponds, as well as for glulam, to mode IV. For the remaining chestnut samples the same failure occurred and for that reason it was not found important to show images of all samples. To prove the uniformity of the results, the load-displacement curves are also presented for all specimens tested in figure 4.44.

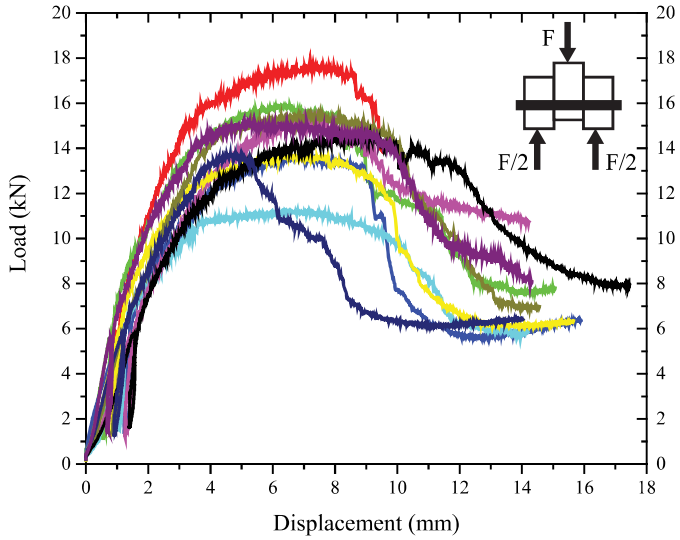

Figure 4.44: Load-displacement curve for selected specimen.

Figure 4.45: Cross-section.

4.4.1.3 CLT

The test procedure was performed according to the monotonic test result (see figures 4.46(a) and 4.46(b)). The maximum load achieved in monotonic test was 12,34 kN, which was the basis to set the procedure according to EN-26891 (1991).

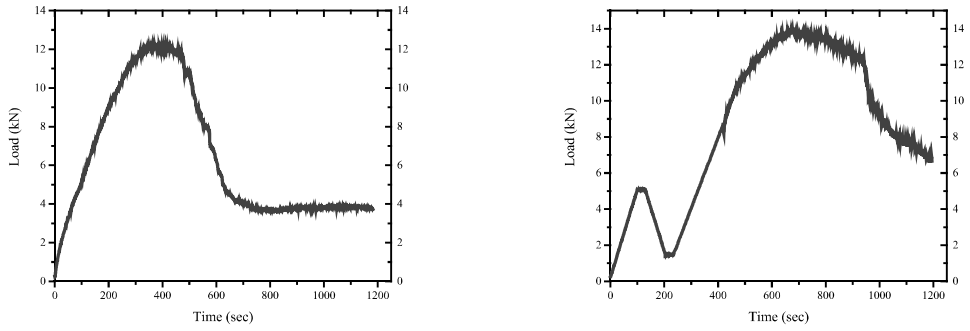

(a) (b)

Figure 4.46: Load-time curves: a) monotonic test; b) procedure.

Analysing the load-displacement curve, presented in figure 4.47, and, at the same time, the physical deformation, in figure 4.49, the most important conclusion that can be reached is the formation of two plastic hinges. After the load-peak, the load-carrying capacity of the dowel started to decrease and consequently the plastic hinges were formed.

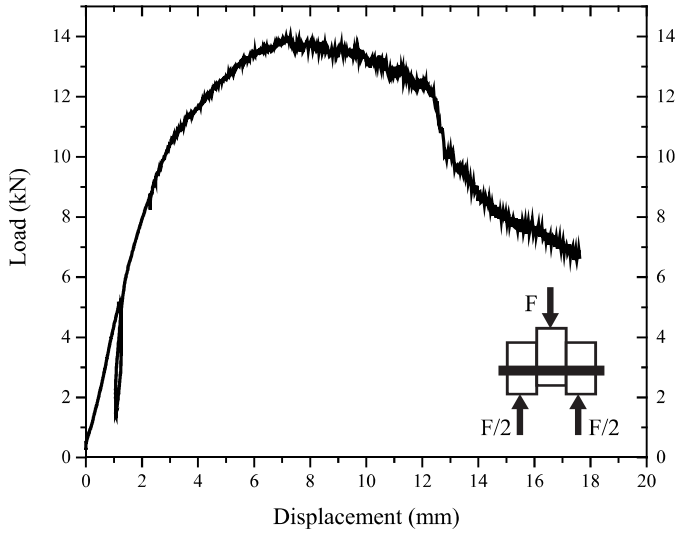

Figure 4.47: Load-displacement curve for selected specimen.

The global behavior of specimens can be analysed in figure 4.48 where low variability (less than 10%) and good uniformity of the results can be noticed.

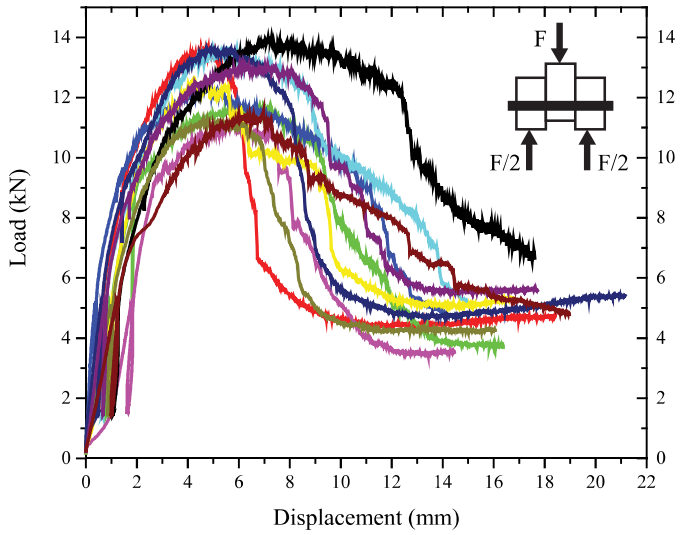

Figure 4.48: Load-displacement curve for selected specimen.

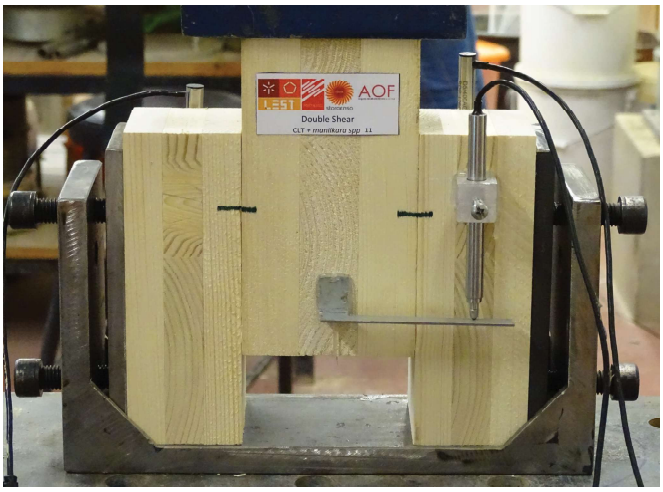

(a)

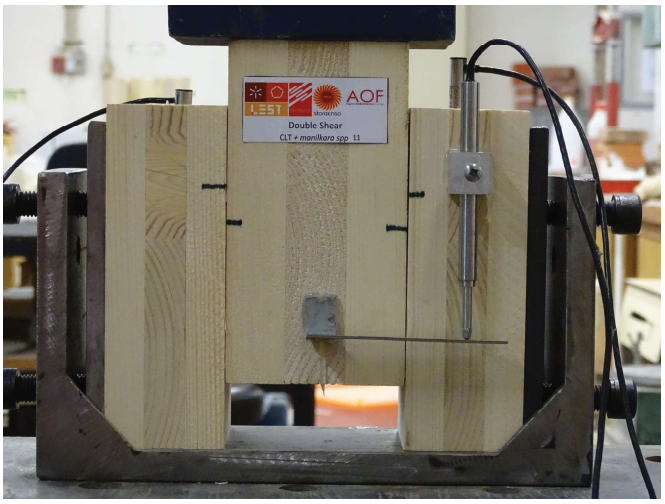

(b)

Figure 4.49: CLT images before and after testing with steel dowel: a) before; b) After.

4.4.2 Comparison between experimental and analytical results

In this subsection the experimental results will be compared with the design rules contained in EN-1995-1-1 (2004). The load carrying capacity for experimental results is given by equation 3.8. Analysing table 4.3, it can be concluded that the failure mode prediction is well adapted. However, by confronting the experimental and analytical results lower values are noted if using EN-1995-1-1 (2004) design rules. This means the underestimation of the load carrying capacity per shear plane per fastener. By means of the timber member used, less variability in engineered wood products was noticed which reinforced the well adapted material characteristics for structural elements (figure 4.50).

Table 4.3: Experimental results vs analytical results based on EC5

Sample	Fmax (kN) (experimental results)	Experimental failure mode	My (N.mm) (analytical result)	F_v,R (kN) (analytical results)	Theoretical failure mode
Glulam (COV)	11,39 (6,63%)	IV	314,14	0,635	IV
Chestnut (COV)	14,72 (11,38%)	IV		0,863	IV
CLT (COV)	12,60 (8,08%)	IV		0,669	IV

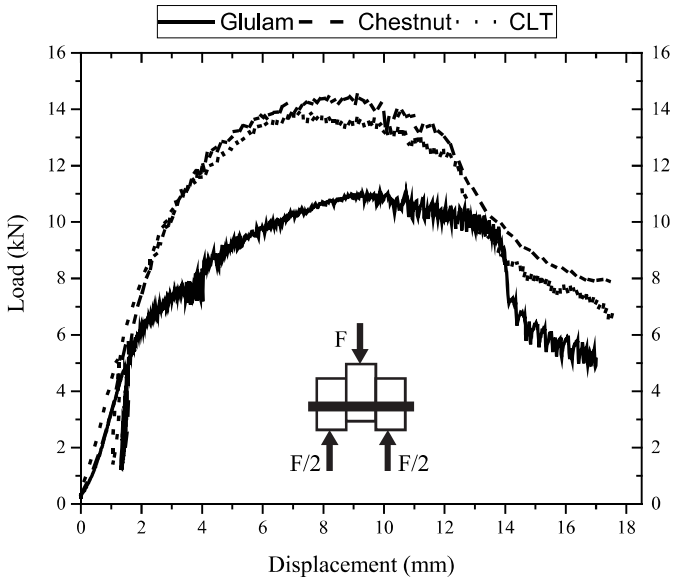

Figure 4.50: Comparison between load-displacement curves for glulam, chestnut, and CLT.

Chapter 5

Summary and Conclusions

5.1 Sumary

Experiments were carried out in the University of Minho, with the aim to study load carrying capacity of wood dowels as well to access the accuracy of EN-1995-1-1 (2004) design formulas.

5.2 Conclusions

Experimental efforts as well as *in situ* observations permitted to conclude good performance of massaranduba dowels and some pleasant plasticity of joints. However a high discrepancy between experimental results and design formulas was found. Thus, the main conclusion of this thesis is the underestimation of EN-1995-1-1 (2004) design formulas concerning wood dowels that unnecessarily lead to undesirable wood construction budget rise. For that reason many experimental and numerical studies need to be done in order to update the standard and transform wood construction even more desirable to humanity.

5.3 Limitations

This thesis study focused only on one type of hardwood as dowel (massaranduda) with 12% of moisture content. Its important to get knowledge about the behavior of other types of softwood and hardwood and with different moisture contents in order to obtain a large database of results.

The monotonic tests is other limitation. This has to do with the importance of studying the behavior of wood dowels under cyclic loads and in a long term.

5.4 Future Work

As already mentioned, a lot of work needs to be done in order to update the existent design formulas. Thus, it is proposed to experimentally study other types of wood dowels and timber members within bigger experimental campaigns. There are a lot of possibilities and variables that need to be done from softwood to hardwood including modern wood products.

Full-scale tests and cyclic-tests with wood connectors should also be done in order to assess the behaviour of wood dowels under such loading conditions.

On the other hand, numerical studies are needed to enlarge the representativeness of the experimental campaign and to reduce the number of variables to be assessed through tests. Only after, it will be possible to propose simplified models and design equations taking into account the fact that the dowel is made of wood instead of the traditional steel considered in the European Yield Model adopted by the current guidelines and design recommendations.

Bibliography

ASTM-D2395 (2014). Standard test methods for density and specific gravity (relative density) of wood and wood-based materials. Technical report.

Barbosa, S. I. F. (2015). Reforço de ligações tradicionais de madeira.

Batchelar, M. and Mcintosh, K. (1988). Structural joints in glulam. In *Proceedings of the 5th World conference in Timber Engineering, Montreux*, volume 4, pages 289–296.

Benson, T. (1981). *Building the Timber Frame House: The Revival of a Forgotten Craft*. Simon and Schuster.

Branco, J. M. (2008). Influence of the joints stiffness in the monotonic and cyclic behaviour of traditional timber trusses. assement of the efficaccy of different strengthenning techniques.

Branco, J. M. and Descamps, T. (2015). Analysis and strengthening of carpentry joints. *Construction and Building Materials*, 97:34–47.

Brühl, F., Kuhlmann, U., and Jorissen, A. (2011). Consideration of plasticity within the design of timber structures due to connection ductility. *Engineering structures*, 33(11):3007–3017.

BS-373 (1957). British standard: Methods of testing small clear specimens of timber. Technical report.

Conrad, M. P., Smith, G. D., and Fernlund, G. (2007). Fracture of wood composites and wood-adhesive joints: a comparative review. *Wood and fiber science*, 36(1):26–39.

Ehlbeck, J. and Larsen, H. (1993). Eurocode 5 - design of timber structures: Joints. *International Workshop on Wood Connectors*, pages 9–23.

Ehlbeck, J. and Werner, H. (1992). Coniferous and deciduous embedding strength for dowel-type fasteners. *Proceedings of CIB-W18*.

EN-1194 (1999). Timber structures - glued laminated timber - strength classes and determination of characteristic values. Technical report.

EN-1995-1-1 (2004). Eurocode 5: Design of timber structures. part 1-1: General, common rules and rules for buildings. Technical report.

EN-26891 (1991). Timber structures. joints made with mechanical fasteners general principles for the determination of strength and deformation characteristics. Technical report.

EN-338 (2003). Structural timber: Strength classes. Technical report.

EN-383 (2007). Timber structures-test methods-determination of embedment strength and foundation values for dowel type fasteners. Technical report.

EN-384 (2004). Structural timber - determination of characteristic values of mechanical properties and density. Technical report.

EN-409 (2009). Timber structures – Test methods – determination of the yield moment of dowel type fasteners – nails. . *European Committee for Standardization.*

Energy, E. (2010). Wood as a sustainable building material.

Erman, E. (1999). A survey on structural timber joint classifications and a proposal taxonomy. *Architectural Science Review*, 42(3):169–180.

Falk, A., Dietsch, P., and Schmid, J. (2016). Proceedings of the joint conference of cost actions fp1402 & fp1404 cross laminated timber: A competitive wood product for visionary and fire safe buildings. In *Joint Conference of COST Actions FP1402 & FP1404 Cross Laminated Timber*. KTH Royal Institute of Technology.

Fujita, K., Nishihama, J., and Shin, E. (2016). Structural characterization os traditional japanese column and penetrating beam joint.

Herzog, T., Natterer, J., Schweitzer, R., Volz, M., and Winter, W. (2004). *Timber construction manual*. Walter de Gruyter.

Hübner, U., Bogensperger, T., and Schickhofer, G. (2008). Embedding strength of european hardwoods. In *CIB-W18 Meeting*, volume 41.

Hunger, F., Stepinac, M., Rajčić, V., and van de Kuilen, J.-W. G. (2016). Pull-compression tests on glued-in metric thread rods parallel to grain in glulam and laminated veneer lumber of different timber species. *European Journal of Wood and Wood Products*, 74(3):379–391.

IGPAI (1973). NP-618-Ensaio de Compressão Axial-1973.pdf. Technical report.

Jensen, J. L., SASAKI, T., and KOIZUMI, A. (2004). Moment-resisting joints with hardwood dowels glued-in parallel to grain. In *Proc., 8th World Conf. on Timber Engineering (WCTE 2004)*, pages 14–17. June.

Johansen, K. (1941). Forsøg med trœforbindelser. *Bygningsstatiske meddelelser*.

Johansen, K. (1949). Theory of timber connections. In *International Association of Bridge and Structural Engineering*, volume 9, pages 249–262.

Madhoushi, M. and Ansell, M. P. (2008a). Behaviour of timber connections using glued-in gfrp rods under fatigue loading. part i: In-line beam to beam connections. *Composites Part B: Engineering*, 39(2):243–248.

Madhoushi, M. and Ansell, M. P. (2008b). Behaviour of timber connections using glued-in gfrp rods under fatigue loading. part ii: Moment-resisting connections. *Composites Part B: Engineering*, 39(2):249–257.

Malo, K., Abrahamsen, R., and Bjertnæs, M. (2016). Some structural design issues of the 14-storey timber framed building "treet" in norway. *European Journal of Wood and Wood Products*, 74(3):407–424.

McLain, T. E. and Thangjitham, S. (1983). Bolted wood-joint yield model. *Journal of Structural Engineering*, 109(8):1820–1835.

Milch, J., Tippner, J., Sebera, V., and Brabec, M. (2016). Determination of the elasto-plastic material characteristics of norway spruce and european beech wood by experimental and numerical analyses. *Holzforschung*.

Mitchell, A. F. (1972). *Conifers in the British Isles. Forestry Commission Booklet Number 33*. Her Majesty's Stationery Office.

Nicolaidis, A., Emberley, Richard and, F.-D., and Torero, J. (2016). Thermally driven failure mode changes in bonded timber joints.

of Threatened Species, I. R. L. (2016).

Parisi, M. A. and Cordié, C. (2010). Mechanical behavior of double-step timber joints. *Construction and Building Materials*, 24(8):1364–1371.

Pizzi, A., Leban, J.-M., Kanazawa, F., Properzi, M., and Pichelin, F. (2004). Wood dowel bonding by high-speed rotation welding. *Journal of adhesion science and technology*, 18(11):1263–1278.

Ross, R. J. et al. (2010). Wood handbook: Wood as an engineering material.

Sandhaas, C., Ravenshorst, G., Blass, H., and van de Kuilen, J. (2013). Embedment tests parallel-to-grain and ductility aspects using various wood species. *European Journal of Wood and Wood Products*, 71(5):599–608.

Sawata, K. and Yasumura, M. (2002). Determination of embedding strength of wood for dowel-type fasteners. *Journal of Wood Science*, 48(2):138–146.

Schmidt, R. (2006). Timber wood dowels consideration for mortise and tenon joint design. *Wood Design Focus*, 14(3):44–47.

Serafini, A., Riggio, M., and González-Longo, C. (2016). A database model for the analysis and assessment of historic timber roof structures. *International Wood Products Journal*, pages 1–6.

Serrano, E. (2000). *Adhesive joints in timber engineering. Modelling and testing of fracture properties.* Lund University.

Snow, M., Asiz, A., Chen, Z., and Chui, Y. H. (2006). North american practices for connections in wood construction. *Progress in Structural Engineering and Materials*, 8(2):39–48.

Sobon, J. A. and Schroeder, R. (2012). *Timber Frame Construction: All about Post-and-Beam Building.* Storey Publishing.

Šobra, K., Avez, C., Aktaş, Y. D., de Rijk, R., Burawska, I., and Branco, J. M. (2016). Load-bearing capacity of traditional dovetail carpentry joints with and without dowels: comparison of experimental and analytical results. In *Historical Earthquake-Resistant Timber Framing in the Mediterranean Area*, pages 215–226. Springer.

Sobra, K., Ferreira, C. F., Riggio, M., D'Ayala, D., Arriaga, F., and Jose-Ramon, A. (2015). A new tool for the structural assessment of historic carpentry joints.

Soltis, L. A., Hubbard, F. K., and Wilkinson, T. L. (1986). Bearing strength of bolted timber joints. *Journal of Structural Engineering*, 112(9):2141–2154.

Standard, J. A. (2003). Japanese agricultural standard for structural glued laminated timber. *JAS, Japanese Plywood Inspection Corporation (JPIC), Tokyo*.

Tanahashi, H. and Suzuki, Y. (2016). Structural mechanisms and deformability of major types of traditional timber joints in japan.

Tannert, T., Vallée, T., and Hehl, S. (2012). Experimental and numerical investigations on adhesively bonded timber joints. *Wood science and technology*, 46(1-3):579–590.

Tong, L. and Steven, G. P. (1999). Analysis and design of structural bonded joints. Technical report, Univ. of Sydney, New South Wales (AU).

Whale, L. and Smith, I. (1986). The derivation of design clauses for nailed and bolted joints in eurocode 5. In *CIB-W18 Meeting*, volume 19.

Wilkinson, T. L. (1972). Analysis of nailed joints with dissimilar members. *Journal of the Structural Division*, 98(9):2005–2013.

This page intentionally left blank.